พีเอ็นเอที่ตรึงบนกระดาษสำหรับการตรวจวัดดีเอ็นเอ

นายณัฐพล จิระกิตติวุฒิ

วิทยานิพนธ์นี้เป็นส่วนหนึ่งของการศึกษาตามหลักสูตรปริญญาวิทยาศาสตรมหาบัณฑิต
สาขาวิชาเคมี ภาควิชาเคมี
คณะวิทยาศาสตร์ จุฬาลงกรณ์มหาวิทยาลัย
ปีการศึกษา 2558

PNA IMMOBILIZED ON PAPER FOR DNA DETECTION

Mr. Nuttapon Jirakittiwut

A Thesis Submitted in Partial Fulfillment of the Requirements

for the Degree of Master of Science Program in Chemistry

Department of Chemistry

Faculty of Science

Chulalongkorn University

Academic Year 2015

Thesis Title	PNA IMMOBILIZED ON PAPER FOR DNA DETECTION
By	Mr. Nuttapon Jirakittiwut
Field of Study	Chemistry
Thesis Advisor	Professor Tirayut Vilaivan, Ph.D.
Thesis Co-Advisor	Thanit Praneenararat, Ph.D.

Accepted by the Faculty of Science, Chulalongkorn University in Partial Fulfillment of the Requirements for the Master's Degree

.....Dean of the Faculty of Science
(Associate Professor Polkit Sangvanich, Ph.D.)

THESIS COMMITTEE

.....Chairman
(Associate Professor Vudhichai Parasuk, Ph.D.)

.....Thesis Advisor
(Professor Tirayut Vilaivan, Ph.D.)

.....Thesis Co-Advisor
(Thanit Praneenararat, Ph.D.)

.....Examiner
(Associate Professor Voravee Hoven, Ph.D.)

.....External Examiner
(Choladda Srisuwannaket, Ph.D.)

ณัฐพล จิระกิตติวุฒิ : พีเอ็นเอที่ตรึงบนกระดาษสำหรับการตรวจวัดดีเอ็นเอ (PNA IMMOBILIZED ON PAPER FOR DNA DETECTION) อ.ที่ปรึกษาวิทยานิพนธ์หลัก: ศ. ดร. ธีรยุทธ วิไลวัลย์, อ.ที่ปรึกษาวิทยานิพนธ์ร่วม: อ. ดร. ธนิษฐ์ ปราณีนรารัตน์, 56 หน้า.

ในระยะเวลาหลายปีที่ผ่านมา อุปกรณ์ตรวจวัดดีเอ็นเอที่อาศัยดีเอ็นเอโอลิโกนิวคลีโอไทด์เป็นโพรบ ได้กลายเป็นเครื่องมือที่สำคัญในการวิเคราะห์ดีเอ็นเอ อย่างไรก็ตามการประยุกต์ยังคงประสบปัญหาเรื่องความไวและความจำเพาะเจาะจง หนึ่งในวิธีที่สามารถเพิ่มความจำเพาะเจาะจงนั้นคือการใช้สารเลียนแบบดีเอ็นเอแทนที่โพรบดีเอ็นเอที่ใช้กันทั่วไป เนื่องจากคุณสมบัติที่เหนือกว่าหลายประการ ในบรรดาสารที่นำมาแทนดีเอ็นเอนั้น เอซีพีซีพีเอ็นเอ (acpcPNA) เป็นตัวเลือกหนึ่งที่น่าสนใจเพราะมีคุณสมบัติที่โดดเด่นในแง่ของความเสถียรของลูกผสม (hybrid) ระหว่างพีเอ็นเอและดีเอ็นเอ รวมถึงความจำเพาะเจาะจงต่อดีเอ็นเอ ในงานนี้เอซีพีซีพีเอ็นเอถูกตรึงลงบนกระดาษเซลลูโลสโดยใช้ไดไวนิลซัลโฟน เป็นตัวเชื่อมขวาง โดยที่เอซีพีซีพีเอ็นเอจะทำหน้าที่เป็นโพรบจับยึดดีเอ็นเอที่ถูกนำส่งโดยการให้เคลื่อนที่ไปตามกระดาษโดยอาศัยแรงแคพิลลารี (capillary force) อย่างรวดเร็ว จากนั้นดีเอ็นเอจะถูกย้อมสีด้วย azure A จากผลการทดลอง อุปกรณ์ตรวจวัดดีเอ็นเอนี้สามารถแยกความแตกต่างระหว่างดีเอ็นเอคู่สมและดีเอ็นเอที่มีลำดับเบสผิดไปหนึ่งตำแหน่งได้ แม้ว่าความไวของการวิเคราะห์จะไม่สูงมากนัก (ขีดจำกัดของการตรวจวัด 3.3 พิโคโมล) ซึ่งทางทฤษฎีแล้วค่าสัญญาณควรจะสามารถเพิ่มได้โดยเพิ่มความยาวของดีเอ็นเอที่วิเคราะห์ แต่จากผลการทดลองเบื้องต้น ความยาวของสายดีเอ็นเอที่เพิ่มขึ้นกลับส่งผลให้ความเกะกะเพิ่มขึ้นด้วย ดังนั้นจึงยังการตรวจวัดดีเอ็นเอสายยาวจึงจำเป็นต้องมีการพัฒนาต่อไปอีก โดยสรุปแล้วได้พัฒนาต้นแบบของอุปกรณ์ตรวจวัดดีเอ็นเอแบบแมโครแอเรย์ฐานกระดาษที่มีเอซีพีซีพีเอ็นเอที่ถูกตรึงเป็นโพรบเพื่อการตรวจวัดดีเอ็นเออย่างง่ายและรวดเร็วโดยไม่ต้องอาศัยการติดฉลากใดๆ และให้ความจำเพาะเจาะจงสูง

ภาควิชา เคมี ลายมือชื่อนิสิต .....

สาขาวิชา เคมี ลายมือชื่อ อ.ที่ปรึกษาหลัก .....

ปีการศึกษา 2558 ลายมือชื่อ อ.ที่ปรึกษาร่วม .....

5671957223 : MAJOR CHEMISTRY
KEYWORDS: DNA SENSOR / ACPCPNA

NUTTAPON JIRAKITTIWUT: PNA IMMOBILIZED ON PAPER FOR DNA DETECTION. ADVISOR: PROF. TIRAYUT VILAIVAN, Ph.D., CO-ADVISOR: THANIT PRANEENARARAT, Ph.D., 56 pp.

In the past few years, DNA sensors based on immobilized DNA oligonucleotides have become an essential tool in DNA analysis. However, sensitivity and selectivity were still problematic in many applications. One efficient way to improve the performance of DNA sensors was a replacement of traditional DNA probe by other DNA mimics which possessed superior properties. AcpcPNA is an attractive candidate DNA replacement because of its excellent stability and specificity of the acpcPNA-DNA hybrid. In this work, the acpcPNA was immobilized on cellulose paper by employing divinyl sulfone as a crosslinker. AcpcPNA acting as a capture probe rapidly hybridized with DNA target which was delivered through capillary transport. After that, DNA detection was carried out by simple staining with azure A. The results showed high specificity which can clearly discriminate single-base mismatch although the sensitivity was somewhat low (detection limit was 3.3 pmol). The signal intensity could have been theoretically enhanced by increasing the length of hanging sequence; nevertheless, preliminary experiments suggest that longer sequence led to more steric effect and therefore the detection of very long DNA sequences still requires further development. In conclusion, a prototype of paper-based macroarray with immobilized acpcPNA probes for DNA detection was developed for a simple and rapid label-free DNA detection with high specificity.

Department:	Chemistry	Student's Signature	.....
Field of Study:	Chemistry	Advisor's Signature	.....
Academic Year:	2015	Co-Advisor's Signature	.....

ACKNOWLEDGEMENTS

Firstly, I would like to express my sincere gratitude to my advisor Prof. Dr. Tirayut Vilaivan and my co-advisor Dr. Thanit Praneenararat for the continuous support of my Ph.D study and related research, for their patience, motivation, and immense knowledge. Their guidance helped me in all the time of research and writing of this thesis. Besides my advisor, I would like to thank the rest of my thesis committee: Assistant Professor Dr. Vudhichai Parasuk, Assistant Professor Dr. Vorawee P. Hoven and Dr. Choradda Srisuwannaket, for their insightful comments and encouragement, but also for the hard question which incented me to widen my research from various perspectives. My sincere thanks also go to Science Achievement Scholarship of Thailand and Distinguished Research Professor Grant for an opportunity to study in Master Degree. Without their precious support it would not be possible to conduct this research. I thank members of TV and TP groups for the stimulating discussions, for the safety manners we were reminding together, and for all the fun we have had in the last three years. Last but not the least, I would like to thank my family: my parents and sister for supporting me spiritually throughout writing this thesis and my life in general.

CONTENTS

Page

Page

Page

LIST OF TABLES

LIST OF FIGURES

LIST OF SCHEME

LIST OF ABBREVIATIONS AND SYMBOLS

µL	microliter
µM	micromolar
µmol	micromole
A^{bz}	N^6-benzoyladenine
Ac	acetyl
Ac_2O	acetic anhydride
ACPC	(1*S*,2*S*)-2-amino-1-cyclopentanecarboxylic acid
C^{bz}	N^4-benzoylcytosine
DBU	1,8-diazabicyclo[5.4.0]undec-7-ene
DIEA	diisopropylazodicarboxylate
DMF	*N*,*N*'-dimethylformamide
DNA	deoxyribonucleic acid
DVS	divinyl sulfone
equiv	equivalent
Fmoc	9-fluorenylmethoxycarbonyl
G^{ibu}	N^2-isobutyrlguanine
HATU	*O*-(7-azabenzotriazol-1-yl)-*N*-*N*-*N*'-*N*' tetramethyluronium hexafluorophosphate
HLA	human leukocyte antigen
HPLC	high performance liquid chromatography
Lys	lysine
MALDI-TOF	matrix-assisted laser desorption/ionization-time of flight
nm	nanometer
OPD	*o*-phenylenediamine
PBS	phosphate buffer saline
PBST	phosphate buffer saline with 0.0005% Tween20
PCR	polymerase chain reaction

PDITC	1,4-phenylenediisothiocyanate
Pfp	pentafluorophenyl
pmol	picomole
PNA	peptide nucleic acid
QPDMAEMA	quaternized poly(2-(dimethylamino)ethylmethacrylate)
RNA	ribonucleic acid
ssDNA	single stranded deoxyribonucleic acid
SA-HRP	streptavidin-horseradish peroxidase
TAE	Tris-acetate-EDTA
TAMRA	tetramethylrhodamine

CHAPTER I

INTRODUCTION

1.1 DNA detection in pattern of analytical array

DNA detection has been very important in the fields of forensic science,[1] food analysis,[2] and diagnostic applications.[3-5] Among various analytical methods, DNA arrays are one of the most attractive methods due to its high throughputness and short detection time. Furthermore, a number of these DNA sensors have been developed and continued to increase in commercial utility.[6] However, they are still not readily accessible for many developing countries, where resources and technology are very limited.[7] Simple and robust assays that can be used routinely and do not require expensive instruments and specially trained personnel are accordingly essential and progressively utilized in those countries. This matter challenges many researchers to develop practical, low-cost, instrument-free and highly effective approaches. In this regard, cellulose paper, a natural material possessing several advantages such as low cost and biocompatibility, is attractive to be employed as an inexpensive platform for such analytical devices.[8-9]

1.2 Background and examples of paper-based analytical devices

The history of paper-based sensors has been dated back since paper chromatography was invented leading to the Nobel Prize in chemistry in 1952.[10-11] Pregnancy test which is a well-known commercial product was produced afterwards. This became the first lateral flow assay and one of the most used point-of-care biosensors.[12] Later, the number of paper-based analytical devices has increased significantly.[10-11] While the majority of DNA arrays employed glass slides, nylon membranes and gold surfaces, paper-based platforms did not gain much attention until recently. During the past 5 years, there were extensive development of paper-based analytical devices in the field of point-of-care DNA testing, where simplicity, affordability, sensitivity, specificity, rapidity and robustness are all required.[13] An example was paper-based analytical devices for DNA detection prepared by a simple

two-step method, in which divinyl sulfone (DVS) was employed as an effective linker.[9]

The DVS molecule contains two electrophilic vinyl groups that allow the covalent attachment of nucleophile-bearing biomolecules.[9] Amino-functionalized oligonucleotides can be immobilized onto cellulose paper through a simple two-step method performed in aqueous solution (**Figure 1.1A)**. Oligonucleotide **A** was spotted onto DVS-activated (DVS+) and unmodified (DVS-) cellulose membranes, which illustrate covalent attachment to the DVS+ substrate and physisorption to the DVS- cellulose respectively (**Figure 1.1B**). Washing step removed the majority of physisorbed oligonucleotide, while covalently-bound DNA remained on the DVS+ membrane. Dylight 649-labeled probe sequence **A'** was utilized in a fluorometric DNA hybridization assay. Oligonucleotide **A** that was bound with DNA on the DVS+ membranes gave stronger signal intensity. This result demonstrated that DVS-activated cellulose paper is suitable to be used as a base material for fabrication of DNA detection device.

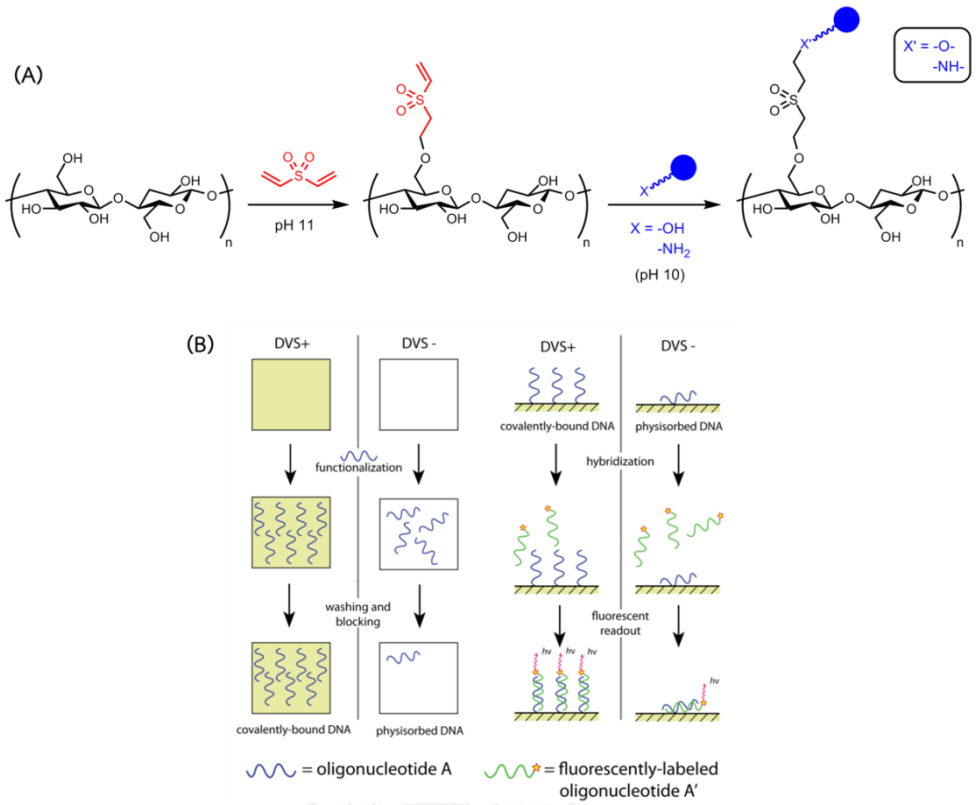

Figure 1.1 (A) Reaction showing chemical activation and functionalization with nucleophile-bearing biomolecule of cellulose. (B) Schematic diagrams of comparison between covalently-bound and physisorbed DNA on cellulose platform for DNA analysis.[9]

Another example is the development of colorimetric bioassay based on cellulose paper to detect the DNA of pathogens. In this study, the paper-based device was prepared by tosylation and precipitation of microcrystalline cellulose; A 5'-end hexanethiol-modified oligonucleotide was then immobilized onto the tosylated cellulose (**Figure 1.2**).[14] After that, the strip was incubated in a solution of biotinylated DNA target, followed by a detection method based on streptavidin-horseradish peroxidase (SA-HRP) using 3,5,3',5'-tetramethylbenzidine as a substrate. The results showed that the detection limit was 0.05 pmol and analysis of 71 and 74 bp PCR products was successful; nevertheless, the specificity was rather low in discrimination between fully matched, single-, double-, and triple-base mismatched sequences.

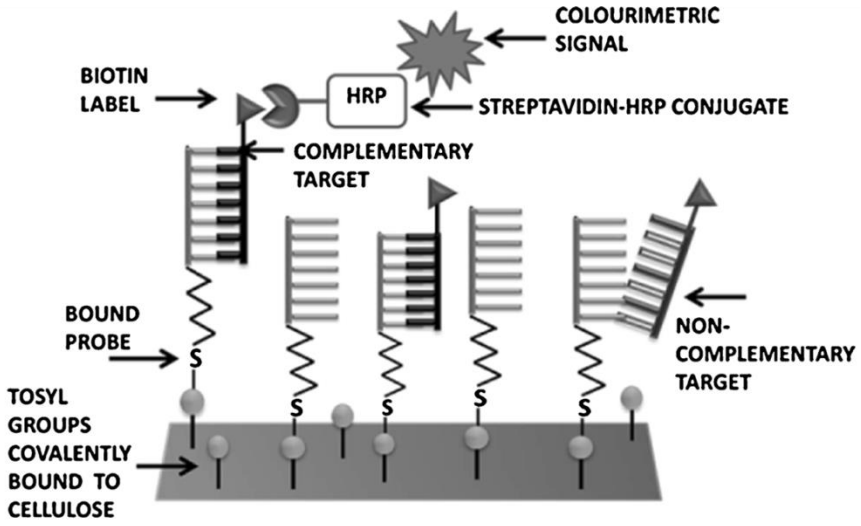

Figure 1.2 Enzyme-based coloricmetric assay on tosylated cellulose paper with immobilized DNA probe.[14]

Another interesting example is the development of a paper-based device for rapid target hybridization. In this work, 1,4-phenylenediisothiocyanate (PDITC), an amine-reactive homobifunctional linker, was used to activate paper sheets for immobilization of amino-functionalized single-stranded DNA (ssDNA) probe (**Figure 1.3A**).[8] The DNA hybridization assay was performed through capillary transport of the DNA sample through the ssDNA-immobilized paper. Importantly, the intrinsic porosity of cellulose paper is a crucial factor which allows capillary flow leading to rapid hybridization. After separation of targeted Cy3-labeled single-stranded DNA from PCR mixture, the strip was dipped in the DNA solution which sequentially moved along the paper. The labeled-target captured by the DNA probe provided fluorescence signals in the area that contain the immobilized probe (**Figure 1.3B**). A similar strategy was also applied with paramagnetic beads-biotinylated PCR products conjugates, which allowed direct visualization by naked eyes (**Figure 1.3C**).[13]

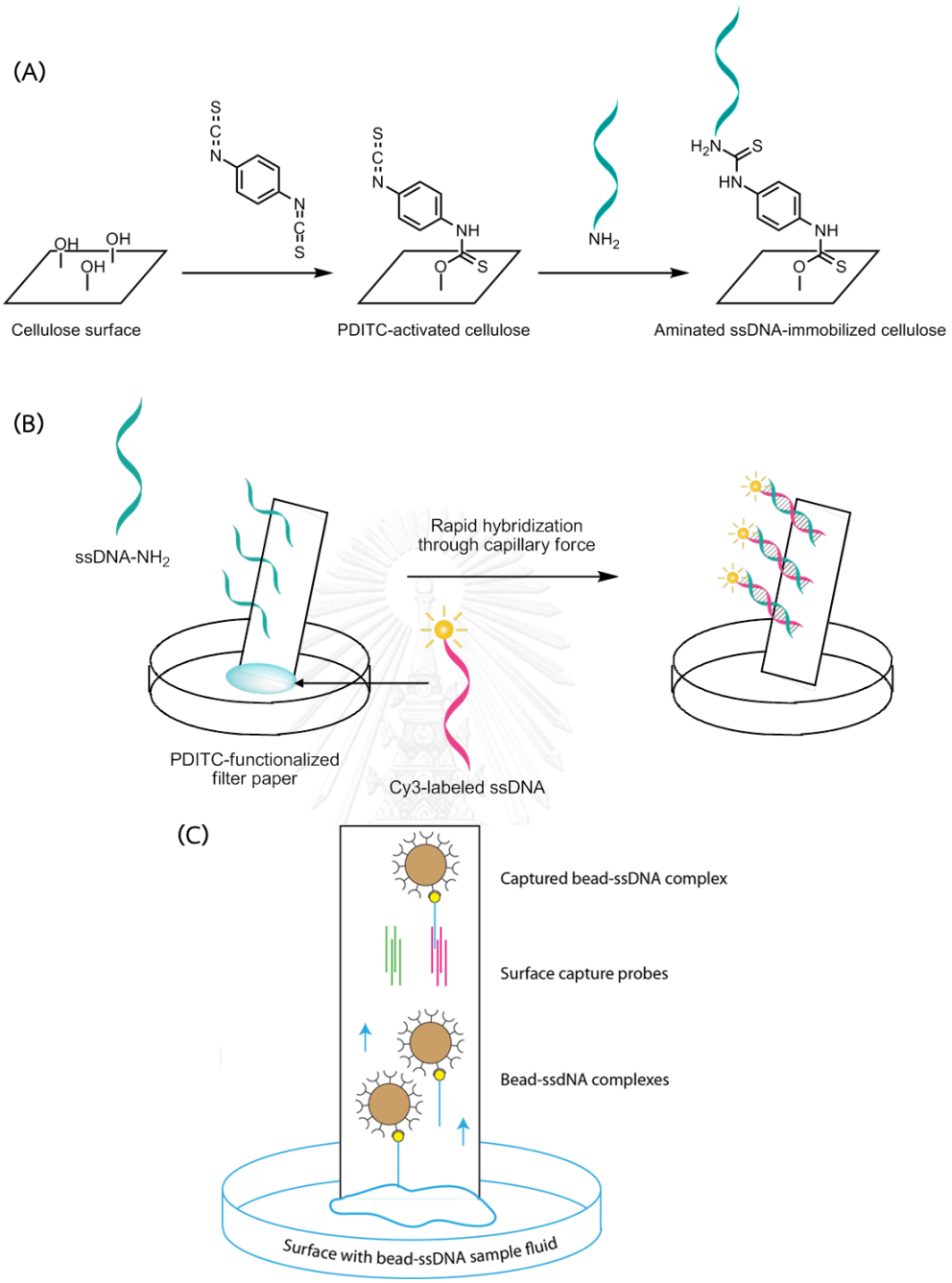

Figure 1.3 (A) Schematic illustration of the methodology of activation of cellulose sufaces with PDITC followed by DNA immobilization. Rapid hybridization of (B) Cy3-labeled ssDNA and (C) bead-ssDNA complexes through capillary force.[8, 13]

Although DNA arrays are widely used and can be applied in several detection assays, the discrimination of single nucleotide mismatch is often challenging.[15] In order to overcome this limitation, peptide nucleic acid, a DNA mimic with remarkable features, especially high specificity, has been extensively investigated as a DNA probe. To the best of our knowledge, the combination of PNA and paper-based device for DNA detection has not yet been reported prior to this study apart from only one report from our own group.[16]

1.3 Peptide nucleic acid

1.3.1 History of peptide nucleic acid and its property

Peptide nucleic acid (PNA) is a nucleic acid analog of which the sugar phosphate backbone is replaced by a synthetic peptide backbone, resulting in an uncharged mimic (**Figure 1.4A**). The PNA prototype, where the backbone consists of *N*-(2-aminoethyl)glycine units (now known as aegPNA) was discovered by Nielsen and coworkers in 1991.[17-19] In spite of the difference of chemical functionalities, the intramolecular distances between consecutive nucleobases and the distance between the nucleobases and the backbone are similar to those in natural DNA molecule.[20] AegPNA consequently can bind to DNA according to standard Watson-Crick rules (**Figure 1.4B**). Due to the absence of charges on aegPNA backbone, electrostatic repulsion between aegPNA-DNA complexes is absent, leading to higher thermal stability than DNA-DNA duplexes. The strong affinity between aegPNA and DNA target usually led to a decrease in the limit of detection in many applications.[2, 15] Another attractive feature of aegPNA is its capability of discriminating between fully matched and single-base mismatched DNA with high specificity – usually exceeds the corresponding DNA. Furthermore, the unnatural peptide backbone of aegPNA exhibits much greater biological and chemical stability than DNA, rendering long-term storage at room temperature and can be used with samples containing proteases or nucleases.[2, 21]

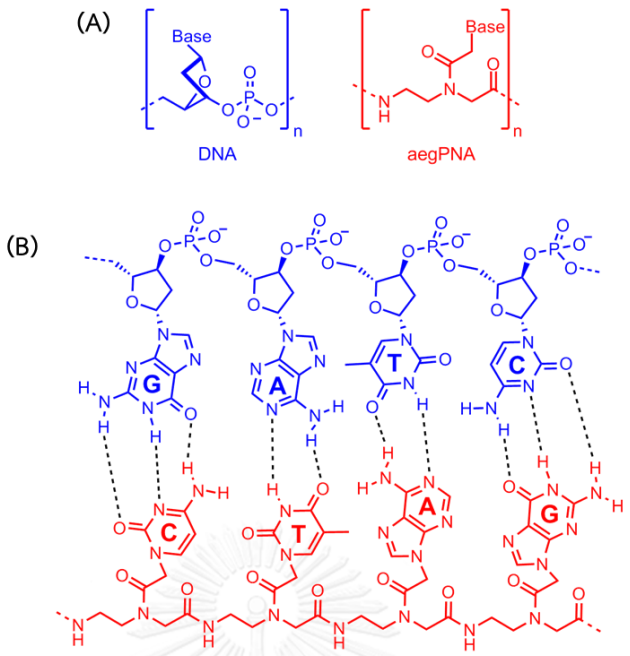

Figure 1.4 (A) Repeating units in the structure of DNA and aegPNA. (B) an aegPNA-DNA duplex in the antiparallel mode, showing the base pairing according to the Watson-Crick base-pairing rules.

Due to the aforementioned advantages, aegPNA has been utilized in various analytical applications, especially for the detection of DNA/RNA targets.[2, 15] Examples include a fluorescent DNA probe based on immobilized aegPNA on a glass slide,[21-22] an aegPNA-immobilized nylon membrane for luminescence imaging,[23] and a label-free DNA detection by using gold nanoparticle enhancement.[24] These developments DNA-based biosensors focused on glass, nylon and gold surface,[25] whereas cellulose platform was rarely applied.

1.3.2 A recent development of conformationally constrained PNAs and their attractive features

Various systems of PNA are being continuously developed in order to improve binding properties over aegPNA, the firstly discovered PNA. One of the most successful concepts is a design of conformationally constrained structure to reduce the entropy change in formation of PNA-DNA complex. Based on this concept, the pyrrolidinyl PNA incorporated with nucleobase-modified proline and 2-amino-1-cyclopentanecarboxylic acid (ACPC) as a rigid spacer (acpcPNA, **Figure 1.5A**) was introduced by Vilaivan and coworkers.[26] AcpcPNA structure is conformationally rigid, rendering higher thermal stability of its DNA hybrid compared to aegPNA. Besides, the specificity of acpcPNA was demonstrated by the extremely large decreases of thermal stability in mismatched hybrids compared to the complementary hybrid. Interestingly, acpcPNA-DNA hybrid could only form in antiparallel direction (**Figure 1.5B**), whereas both parallel and antiparallel forms may occur in aegPNA-DNA hybrids. The excellent performance of acpcPNA suggests it as a potential candidate as a paper-based analytical device for DNA detection with improved sensitivity and specificity.

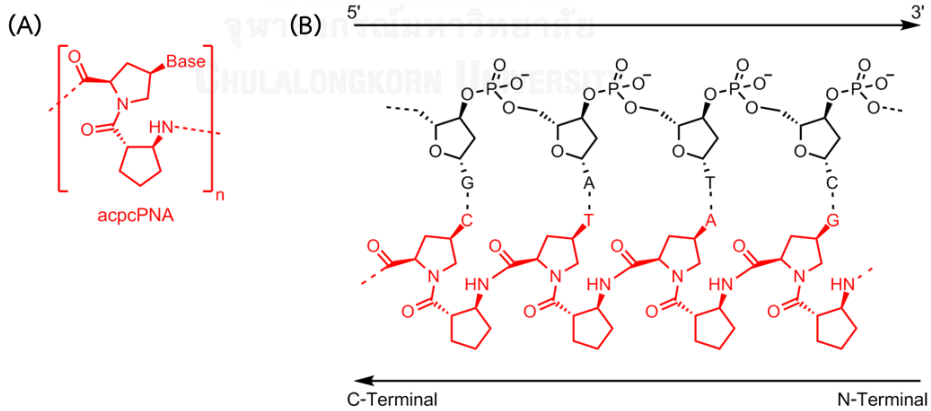

Figure 1.5 (A) acpcPNA structure. (B) Antiparallel hybrid of acpcPNA and DNA.

A potential prototype of paper-based DNA biosensors using acpcPNA probe was described by Laopa and coworkers.[16] The development of this sensor is based on the concept similar to dot blot hybridization that consists of four steps, which are spotting of the DNA targets on the paper substrate ("blotting"), hybridization with sequence-specific probe, conjugation to enzyme-labeled secondary probe, and addition of substrates to generate signals. For the first step, DNA target was spotted on cellulose paper functionalized with a positively charged polymer called quaternized poly(2-(dimethylamino)ehtylmethacrylate) or QPDMAEMA. The DNA was adsorbed on the membrane by electrostatic interaction between the positive charges of the QPDMAEMA-grafted paper and the negative charges of its backbone phosphate groups. The immobilized DNA was then hybridized with biotinylated acpcPNA probe (b-PNA) and sequentially conjugated with streptavidin-horseradish peroxidase (SA-HRP), whereas mismatched DNA was not (**Figure 1.6**). Finally, a yellow signal was generated by the reaction with the HRP substrates – *o*-phenylenediamine (OPD) and hydrogen peroxide. This enzyme-based colorimetric assay showed a very high sensitivity where detection limit was 10 fmol. Moreover, incorporation of acpcPNA exhibited high specificity allowing single mismatch discrimination. However, many steps were required and the adsorption of the DNA by electrostatic interaction is non-specific by nature, and therefore other non-specific DNA may potentially interfere with the detection according to this concept.

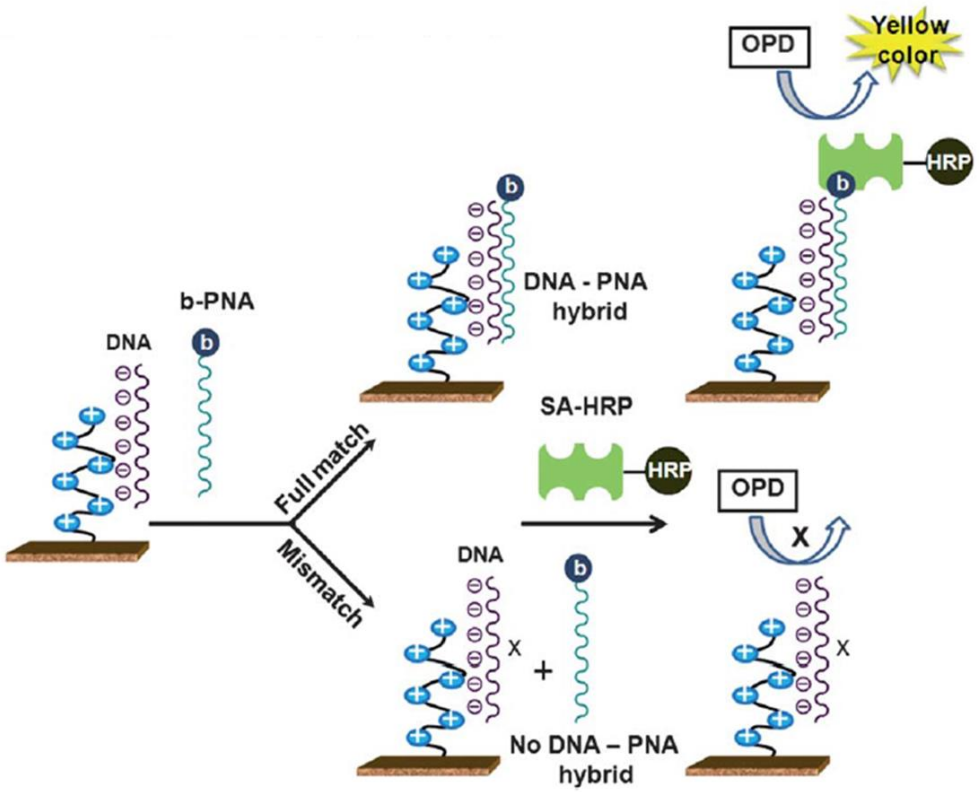

Figure 1.6 Schematic diagram of a paper-based colorimetric enzyme-based assay for DNA detection using acpcPNA probes.[16]

1.4 Rationale and objective of this work

This work aims to develop a paper-based DNA analytical device for point-of-care tests. AcpcPNA possessing high sequence specificity and strong affinity to DNA was employed as a probe. Unlike the previous work by Laopa et al. that also uses acpcPNA and cellulose paper for DNA detection,[16] the acpcPNA probes will be covalently immobilized on the cellulose membrane through a suitable chemistry such as divinyl sulfone activation. This will be used in combination with a simple, rapid, label-free and instrument-free method for the DNA detection with high sensitivity and specificity. Thus, a simple two-step assay consisting of DNA hybridization and staining steps was proposed. The DNA target will be captured by acpcPNA immobilized on cellulose paper *via* capillary transport (**Scheme 1.1A**) and then stained with a suitable cationic dye which would selectively interact with the captured DNA target, but not with the immobilized PNA probe, through electrostatic

interaction (**Scheme 1.1B**). Mismatched DNA would not bind to the immobilized PNA probes and would be easily removed by washing with a buffer solution.

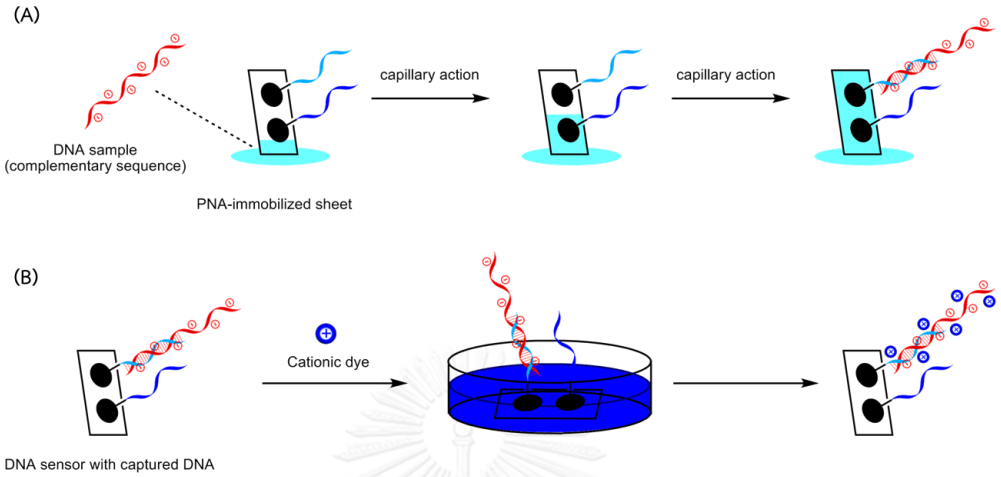

Scheme 1.1 (A) Movement of DNA along paper strip through capillary transport. DNA target was captured by complementary acpcPNA probe and ignored by the other. (B) Electrostatic interactions between a cationic dye and target DNA captured by acpcPNA immobilized on cellulose membrane.

CHAPTER II

EXPERIMENTAL SECTION

2.1 Materials

All chemicals were purchased from Fluka, Merck, ChemImpex or Sigma-Aldrich Chemical Co., Ltd., and were used as received without further purification. Anhydrous *N,N*-dimethylformamide ($H_2O \leq 0.01$ %) for solid phase peptide synthesis was obtained from RCI Labscan and was dried over activated 4Å molecular sieves before use. The solid support for peptide synthesis (TentaGel S-RAM Fmoc resin, 0.24 mmol/g) was obtained from Fluka. The protected amino acids (Fmoc-L-Lys(Boc)-OPfp) were purchased from Calibiochem Novabiochem Co., Ltd. Nitrogen gas was obtained from Labgas (Thailand) Co., Ltd. with high purity up to 99.995%. Chromatography paper (grade 1 Chr) was purchased from GE Healthcare UK Ltd. Divinyl sulfone was purchased from Merck. Azure A was purchased from Chemimpex. MilliQ water was obtained from ultrapure water system with Millipak® 40 filter unit 0.22 µm, Millipore (USA). All oligonucleotides were purchased from Pacific Science (Bangkok, Thailand).

2.2 Synthesis of acpcPNA

2.2.1 AcpcPNA monomer synthesis

The four Fmoc-protected, Pfp-activated pyrrolidinyl PNA monomers (Fomc-A^{Bz}-OPfp, Fmoc-C^{Bz}-OPfp, Fmoc-G^{Ibu}-OH and Fmoc-T-OPfp), and (1*S*,2*S*)-2-amino-1-cyclopentanecarboxylic acid (ACPC) spacer (**Figure 2.1**) were synthesized by Ms. Boonsong Ditmangklo (Fmoc-T-OPfp, Fmoc-ACPC-OPfp), Ms. Duangrat Nim-Anussornkul (Fomc-A^{Bz}-OPfp, Fmoc-C^{Bz}-OPfp) and Mr. Chayan Charoenpakdee (Fmoc-G^{Ibu}-OH) using the previously reported methods.[27-28]

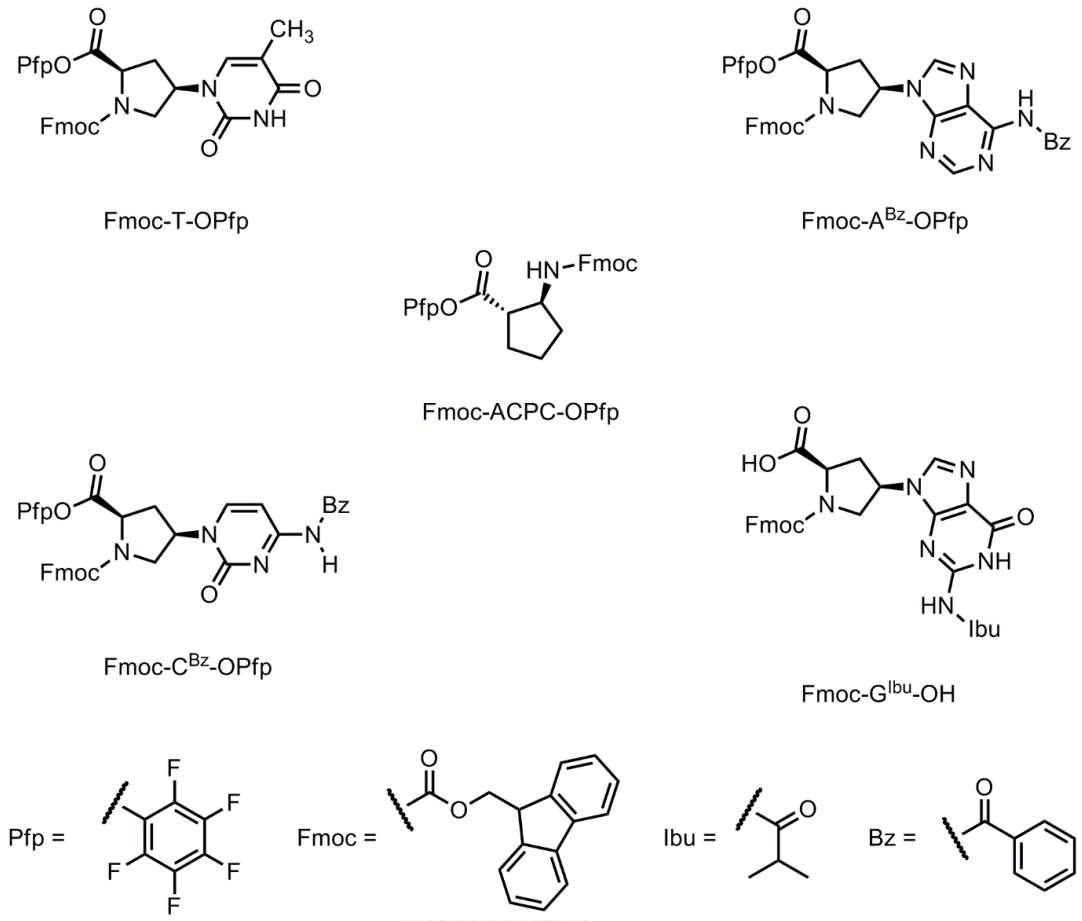

Figure 2.1 Structure of pyrrolidinyl PNA monomers and ACPC spacer used for solid phase peptide synthesis

2.2.2 Solid phase peptide synthesis

AcpcPNAs were synthesized on Tentagel S-RAM resin through a standard solid-phase peptide synthesis protocol at 1.5 μmol scale (1 equiv) by stepwise couplings of four Fmoc-protected pyrrolidinyl PNA monomers and the activated ACPC spacer as reported in details elsewhere.[29] The *N*-terminal Fmoc group on the resin was first removed (100 μL of 20% piperidine and 2% DBU in DMF, 5 minutes), revealing a reactive *N*-terminal amine. Next, Pfp-activated monomers or spacer or Fmoc-L-Lys(Boc)-OPfp were directly coupled to free amino groups on the resin (4 equiv Pfp-activated monomers or spacer or Fmoc-L-Lys(Boc)-OPfp, 4 equiv HOAt, 4 equiv DIEA in DMF, 30-minute single coupling (40 minutes for Fmoc-T-OPfp)). In the case of Fmoc-G^{Ibu}-OH, HATU-activation was required before the coupling

(4 equiv free acid monomers, 4 equiv HATU, 8 equiv DIEA in DMF, 1-minute pre-activation, 40-minute single coupling). Finally, a capping step was applied to ensure the absence of any unreacted free amino group (5 µL of Ac_2O and 30 µL of 7% DIEA in DMF). This process was repeatedly performed until the desired sequence was obtained. For the last amino acid, *N*-terminal Fmoc group was removed and the free amino group of the acpcPNA was then acetylated. The nucleobase protecting groups were removed by heating with 1:1 aqueous ammonia-dioxane at 60 °C overnight, before the resin was washed thoroughly with methanol and dried. The acpcPNA was cleaved by treatment with 500 µL of trifluoroacetic acid (TFA) for 1 hour (3 times), purged by N_2 and washed by diethyl ether to remove TFA. Purification was performed by reverse phase HPLC on a Water 600 HPLC System using C-18 column (4.6x50 mm). The sample elution was carried out using a gradient of water (A) and methanol (B) containing 0.1% trifluoroacetic acid (monitored by UV absorbance at 260 nm, 10% B for 5 minutes then linear gradient to 90% B over 60 minutes, flow rate 0.5 mL/minute). Characterization was achieved by MALDI-TOF mass spectrometry (Microflex, Bruker Daltonics) and purity was analyzed by HPLC (10% B for 5 minutes then linear gradient to 90% B over 35 minutes, flow rate 0.5 mL/minute).

2.3 Fabrication of the acpcPNA macroarray

2.3.1 Divinyl sulfone activation

Cellulose membrane was immersed in divinyl sulfone solution (10 %v/v DVS in 0.1 M Na_2CO_3 buffer, pH 11) and shaken on an orbital shaker for 2 hours. After three-time washing with MilliQ water, the cellulose sheet was air-dried at room temperature.[9] The DVS-activated paper should be used on the same day.

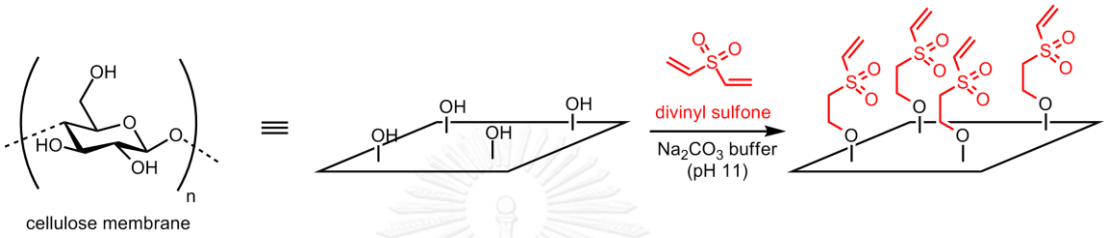

Figure 2.2 Chemical activation of cellulose paper using DVS molecules

2.3.2 Immobilization of acpcPNA on cellulose support

AcpcPNA solution (0.5 µL of 200 µM acpcPNA in phosphate buffer saline (PBS), pH 7.4; equivalent to a total amount of 100 pmol acpcPNA) was spotted onto the DVS-activated paper and the paper was incubated in a humidity chamber for 16 hours. The cellulose sheets were next washed with PBST (phosphate buffer saline with 0.0005%w/v Tween20) solution on an orbital shaker for 1 hour and then air-dried at ambient temperature.

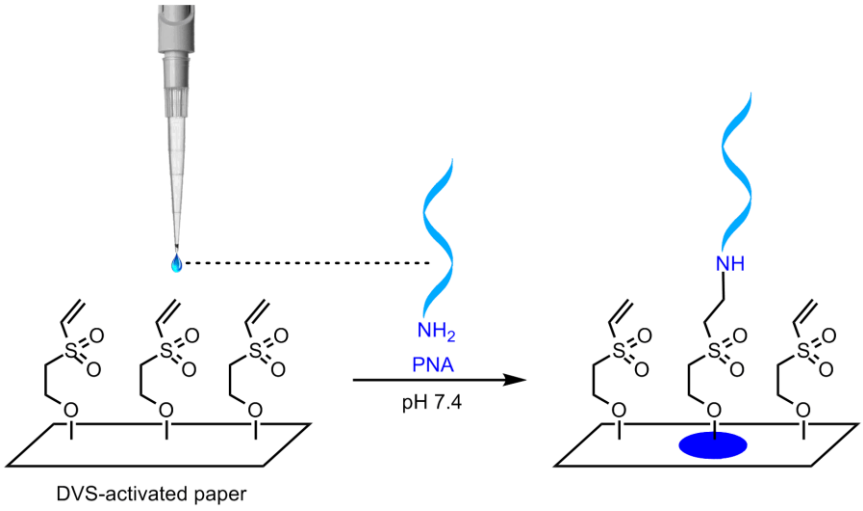

Figure 2.3 Immobilization of acpcPNA on DVS-activated paper.

2.4 Hybridization by capillary transport

After 4 corners of acpcPNA-immobilized strip were cut, it was dipped into a DNA target solution (PBST as a solvent, **Figure 2.4**). The sample was drawn towards the other end of the paper by capillary action. After the whole paper sheet was thoroughly wet, the paper was air-dried at room temperature and then dipped into the solution again, using the opposite end. This was followed by washing with PBST and PBS solution on an orbital shaker for 3 minutes and air-dried before the detection step.

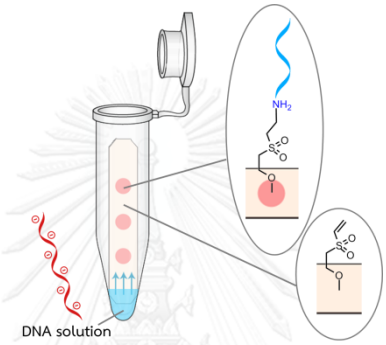

Figure 2.4 DNA hybridization through cappillary force.

2.5 Colorimetric detection

The sheet was immersed in a solution of azure A (1 mg/mL, in MilliQ water) for 30 minutes without shaking, washed with PBS solution twice (3 minutes), and then air-dried. Optical images were obtained by scanning with a multifunction printer (HP Deskjet Ink Advantage 2515) with resolution of 2400 dpi.

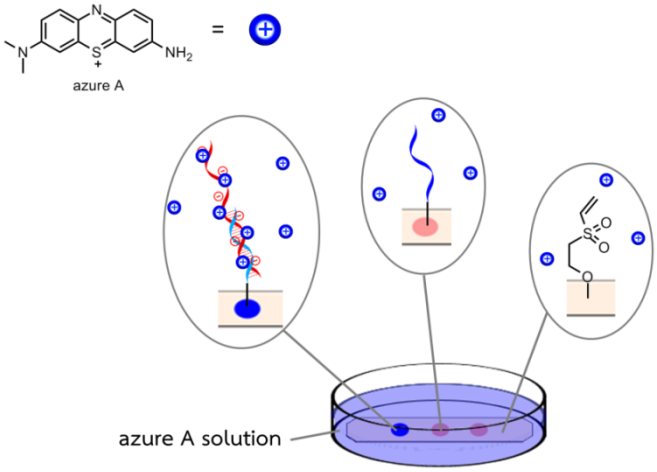

Figure 2.5 Specific binding of azure A and DNA *via* electrostatic interaction.

2.6 Fluorometric detection

2.6.1 Ethidium bromide stain

The sheet was stained with 0.5 μg/mL ethidium bromide in Tris-acetate-EDTA (TAE) buffer (pH 8.0) for 30 minutes without shaking, destained in water for 30 minutes, and then air-dried before taking the image under 365 nm UV light using (Cannon Powershot SX1110IS, camera setting: ISO-100, f/2.8 and 1.3-s exposure time).

2.6.2 SYBR Gold stain

The sheet was stained in a 1:10000 dilution of SYBR Gold stock solution (10000X) in TAE buffer (pH 8.0) for 30 minutes without shaking, destained in water for 30 minutes, and then air-dried before taking the image under 365 nm UV light as above.

2.7 Image Analysis

Images of all tested sensors were scanned by multifunction printer and saved as JPEG files with a resolution of 2400 dpi. Using ImageJ software (National Institutes of Health), the marked areas on the obtained images were selected by the "selection" command (all circled region were exactly the same area in size and smaller than the average size of each area which signal appears to ensure that all measured areas excluded the blank area) and converted to integrated intensity by the "measure" command. The integrated intensity was plotted in the Microsoft Excel.

Fluorescence assay results were obtained by photographing under black light (365 nm) with the following camera setting: ISO-100, f/2.8 and 1.3-s exposure time. The marked areas were analyzed in the same process as colorimetric assay.

For quantitative analysis of various signals, the Student's t-test was employed in Microsoft Excel at p = 0.05. The detection limit was determined to be the concentration that gave no statistical difference between the signals from the respective concentration and the background control.

CHAPTER III

RESULTS AND DISCUSSION

3.1 Synthesis and characterization of acpcPNA oligomer

The acpcPNA oligomers used in this work were T_9, 5801, 5701, R06N and R06M (**Table 3.1**). T_9 was used in DNA-binding test with a fluorescein-labeled DNA oligomer. PNA 5801 was mainly employed in this work including optimization, discrimination and comparison experiments. For PNA 5701, R06N, and R06M, they were used in double- and single-base discrimination experiments. After solid-phase synthesis, 1.5 μmol of resin bearing acpcPNA oligomers was stored at 4 ℃ until they were required. After cleavage of acpcPNAs from resin, they were purified by HPLC and characterized by MALDI-TOF mass spectrometry. All acpcPNAs gave the expected masses and their purities were more than 90%, as confirmed by HPLC (**Figure A1–5**). The concentration was determined by UV spectrophotometry at 260 nm using molecular extinction coefficient values calculated by an in-house web-based software (http://www.chemistry.sc.chula.ac.th/pna). The characterization data of all acpcPNAs was summarized in **Table 3.1**.

Table 3.1 Characterization data of acpcPNA

Name	PNA sequence	t_R[a] (minute)	Yield[c] (%)	Molecular Weight (observed)[b]	Molecular Weight (calculated)
T_9	Ac-TTTTTTTTT-LysNH_2	32.2	35	3186.495	3179.440
5701	Ac-CGCCATCCTCG-LysNH_2	28.9	28	3820.714	3813.121
5801	Ac-CTCCGTCCTCG-LysNH_2	28.2	18	3811.007	3804.108
R06N	Ac-Lys-GCCTCACCACCA-NH_2	28.3	31	4128.241	4123.478
R06M	Ac-Lys-GCCTTACCACCA-NH_2	28.1	8	4143.332	4138.490

[a]See HPLC conditions in experimental section. [b]MALDI-TOF mass spectrometry in linear positive ion mode using α-cyano-4hydroxycinnamic acid as a matrix. [c]Isolated yield after HPLC.

3.2 Preliminary experiment for PNA immobilization

3.2.1 Immobilization of fluorescein-labeled acpcPNA on DVS-activated paper

There are various approaches to immobilize amino-containing acpcPNA probes. However, not all of them are suitable for colorimetric detection proposed in this study. Click chemistry and surface activation using bifunctional molecule such as disuccinimidyl adipate, PDITC and DVS were chosen for the immobilization. Unfortunately, click reaction gave undesired fluorescence signal (**Figure A6–7**), whereas disuccinimidyl adipate-activation which was based on spot synthesis induced inconsistent background after staining with methylene blue solution (**Figure A8–10**). Although immobilization of acpcPNA can be performed through PDITC-activation,[8] there is no signal after detecting DNA with gold nanoparticle staining (**Figure A14**) and many washing steps were also required (**Figure A11–12**). After an extensive screening, DVS chemistry[9] was found to be the most suitable one. To prove that acpcPNA can be covalently attached on the paper, fluorescein-labeled acpcPNA was used since the signal of which can be monitored under black light (**Figure 3.1A**). Comparing between acpcPNA spotted onto the DVS-activated and unmodified cellulose membrane, higher signal intensity of the former demonstrated that acpcPNA was efficiently immobilized on the DVS-activated cellulose paper (**Figure 3.1B**). The presence of signal in negative control arise form non-specific adsorption due to the hydrophobicity of fluorescein label, which is difficult to be washed away by water (**Figure 3.1C**).

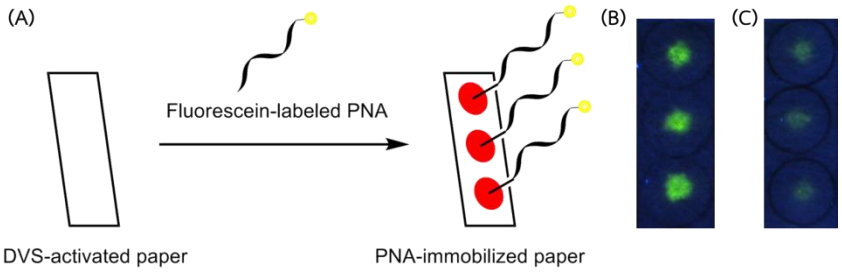

Figure 3.1 (A) The immobilization of fluorescein-labeled acpcPNA (synthesized by Ms. Chotima Vilaivan, sequence: fluorescein-O-CGTCCACGTA-LysNH_2; O = 2-[2-(2-aminoethoxy)ethoxy]acetyl linker) on DVS-activated membrane. Fluorescence images under black light (365 nm) after immobilization of fluorescein-labeled acpcPNA (100 pmol/spot) on (B) DVS-activated and (C) unmodified cellulose membrane.

3.2.2 Binding experiment of unlabeled PNA immobilized on cellulose paper and fluorescently labeled DNA

Rapid hybridization along with multiple detections was carried out through capillary transport,[8] where DNA in aqueous solution was pulled along paper strip via capillary force and then captured by a specific sequence of acpcPNA immobilized on the cellulose membrane (**Figure 3.2A** and **B**). Moreover, there is no non-specific interaction between the DNA and the cellulose paper as sometimes observed when DNA target was directly spotted onto the membrane. To prove this concept, the T_9 acpcPNA probe was first immobilized on the cellulose paper by DVS chemistry. The fluorescently-labeled DNA was then employed as the target, and the binding was observed under black light. Only complementary DNA gave fluorescence signal after washing (**Figure 3.2C–E**). The result confirmed that acpcPNA can perform effectively under this system.

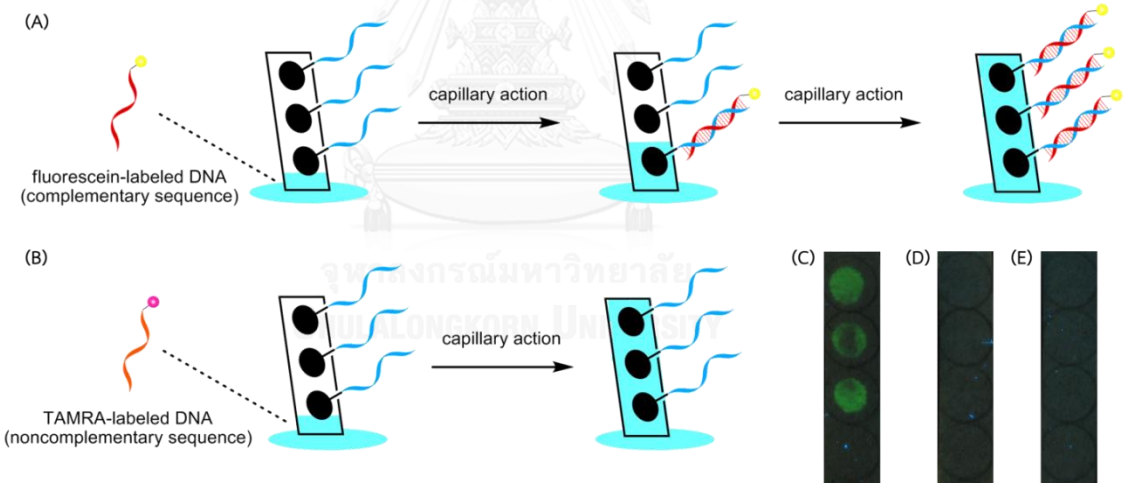

Figure 3.2 (A) The schematic illustration of hybridization of fluorescein-labeled complementary (sequence: 5'-fluorescein-AAAAAAAAA-3', 6 μM) and (B) TAMRA-labeled non-complementary DNA (5'-TAMRA-CGAGGGATAACT-3', 6 μM) to immobilized acpcPNA probe (T9, 100 pmol/spot) by capillary transport. Fluorescence images of acpcPNA macroarray hybridized with (C) fluorescein-labeled complementary and (D) TAMRA-labeled non-complementary DNA and (E) negative control.

3.2.3 Staining with cationic dye

Before focusing on cationic dye, silver (**Figure A13**) and gold nanoparticle staining (**Figure A14**) were studied.[24, 30] Unexpectedly, silver staining showed incontrollable background whereas gold nanoparticle staining was low reproducibility (**Figure A13–14**). To generate a signal from label-free DNA, we proposed that cationic dyes capable of selectively forming electrostatic interaction with negatively charged DNA or PNA-DNA duplexes (**Figure 3.3A**) are likely to be a viable readout. In the experiment, unlabeled PNA 5801 probe was immobilized followed by hybridization with complementary DNA target and staining. After screening various cationic dyes (**Figure A15**) commonly used for DNA staining (methylene blue, azure A, azure II, ethyl violet, and nile blue), azure A provided the highest intensity with lowest amount of non-specific interaction between dyes and probes (**Figure 3.3C** and **D**).

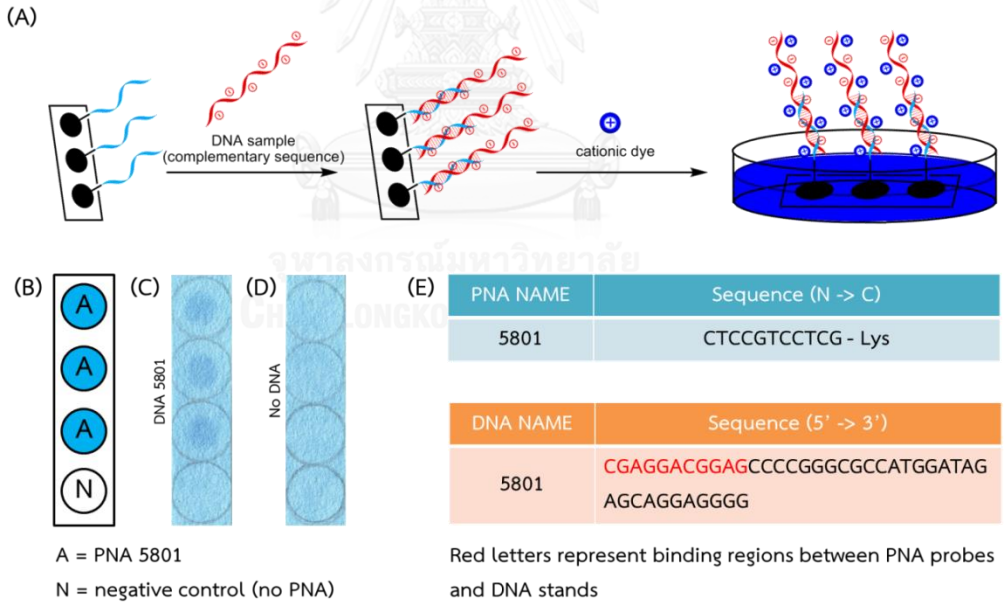

Figure 3.3 (A) The schematic view of two-step DNA detection. (B) Array layout. (C) The scanned images of DNA sensors for HLA-B*5801. (D) Negative control. (E) The tables showing PNA and DNA sequences used in the preliminary experiment.

3.3 Optimization of acpcPNA immobilization and dye staining

3.3.1 Optimal duration to immobilize acpcPNA

In order to determine the minimum required duration of the immobilization step, incubation times were varied from 30 minutes to 16 hours. The hybridization and detection with azure A were then carried out on these membranes to observe immobilization efficiency, as judged by the signal intensity. The signals appeared on the membrane after 4 hours, therefore the minimum duration required for PNA immobilization is 4 hours (**Figure 3.4B**). However, 16-hour incubation was the optimal condition and used as a standard procedure in subsequent studies because of the highest immobilization intensity (**Figure 3.4C**).

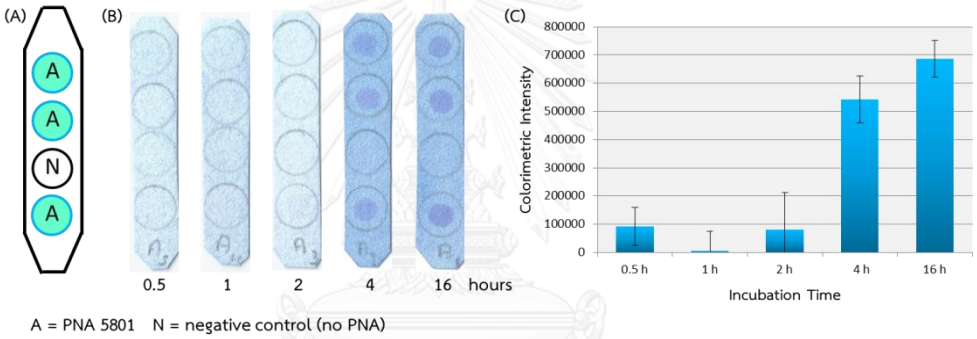

Figure 3.4 (A) Array layout. (B) The scanned images of DNA sensors prepared from different activation times (0.5, 1, 2, 4 and 16 hours). (C) Signal intensities derived from scanned images *via* the software ImageJ.

3.3.2 Optimization of staining time

To investigate optimal staining condition, the acpcPNA-immobilized cellulose membranes after DNA were incubated in azure A solution for different durations from 5 to 60 minutes (**Figure 3.5B**). The signal intensity was low for short incubation periods (5 and 15 minutes), but the background intensity was unacceptably high for too long incubation (60 minutes). Thus, the optimal incubation time is 30 minutes (**Figure 3.5C**).

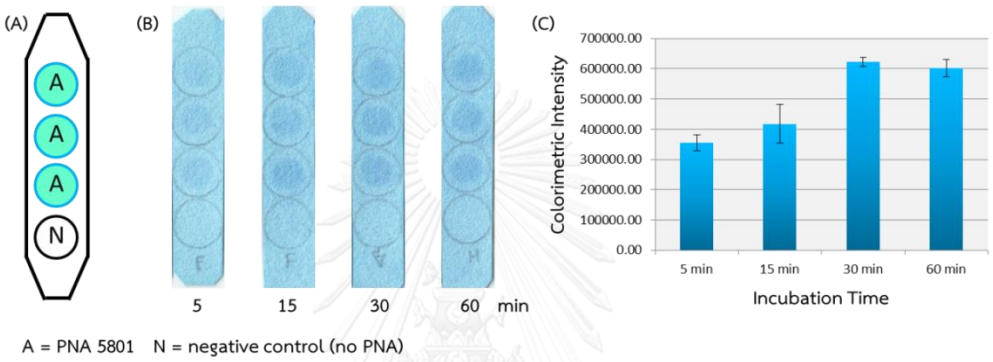

Figure 3.5 (A) Array layout. (B) The scanned images of DNA sensors incubated in azure A solution for different times (5, 15, 30 and 60 minutes). (C) Signal intensities derived from scanned images *via* the software ImageJ.

3.4 Performance of acpcPNA-immobilized cellulose paper as DNA biosensors

3.4.1 Specificity tests

3.4.1.1 Double-bases mismatch discrimination

We created a macroarray of three distinct features, consisting of two different probes and one negative control (**Figure 3.6A**). One probe, called PNA 5701, is specific to a portion of the gene HLA-B*5701, which is strongly related to abacavir hypersensitivity reaction, whereas the other one, called PNA 5801, is specific to the gene HLA-B*5801, a normal variant. The two 11-mer probes are different at two positions (**Figure 3.6E**). The result showed that each probe can specifically bind its complementary DNA sequence with perfect discrimination (**Figure 3.6B and C**).

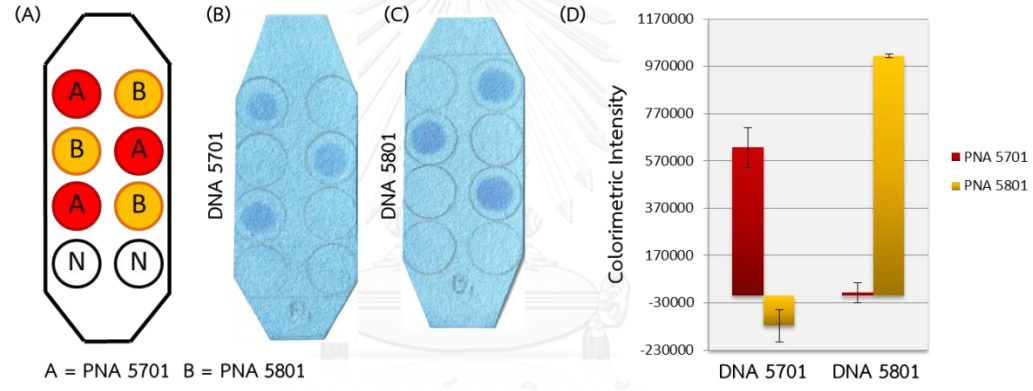

(E)

PNA NAME	Sequence (N -> C)
5701	CGCCATCCTCG - Lys
5801	CTCCGTCCTCG - Lys

Pink letters represent base mismatches.

DNA NAME	Sequence (5' -> 3')
5701	CGAGGACGGAGCCCCGGGCGCCATGGATAGAGCAGGAGGGG
5801	CGAGGATGGCGCCCCGGGCGCCATGGATAGAGCAGGAGGGG

Red letters represent binding regions between PNA probes and DNA stands.

Figure 3.6 (A) Array layout. (B) and (C) the scanned images of DNA sensors for HLA-B*5701 and 5801. (D) Signal intensities derived from scanned images *via* the ImageJ image processing software. (E) The tables showing PNA and DNA sequences used in double-base mismatch discrimination experiment.

3.4.1.2 Single-base mismatch discrimination

3.4.1.2.1 Normal condition

A macroarray similar to the experiment in 3.3.1 was created. One probe, called PNA R06M, specific to DNA R06M which represents a mutated gene at codon 26 of beta thalassemia and the other, called PNA R06N, specific to normal DNA R06N were immobilized in a pattern shown in **Figure 3.7A**. The two 12-mer probes are different at two positions (**Figure 3.7F**). Higher signal intensity on fully-complementary duplexes demonstrated high specificity of acpcPNA, although the signal on the mismatch duplexes was also observed (**Figure 3.7B**). This demonstrated that the discrimination is not optimal for single mismatch discrimination.

3.4.1.2.2 Higher stringency in washing condition

It was proposed that the unsatisfactory single mismatch discrimination was primarily due to the rather high stability of the mismatched PNA-DNA duplexes. To solve the problem of non-specific interaction, we envisioned that addition of an organic solvent, such as acetonitrile, may reduce the stability of the mismatched duplexed. This strategy was successfully used in a related work.[31] The results showed that addition of acetonitrile (20 %v/v in buffer solution) significantly removed the signal of the mismatched PNA-DNA pairs, despite slightly losing signal intensity of the complementary PNA-DNA pairs (**Figure 3.7C**).

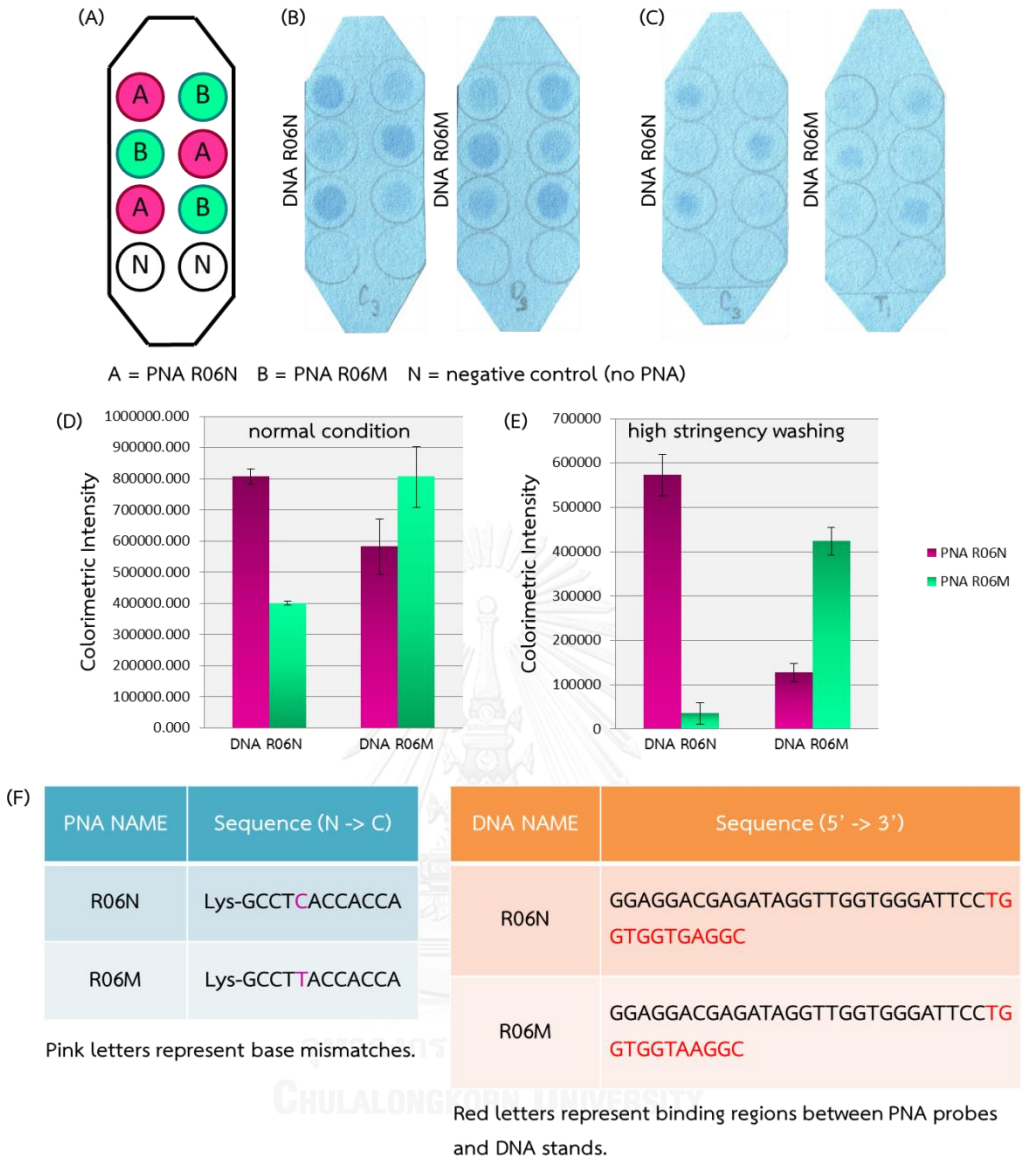

(F)

PNA NAME	Sequence (N -> C)
R06N	Lys-GCCTCACCACCA
R06M	Lys-GCCTTACCACCA

Pink letters represent base mismatches.

DNA NAME	Sequence (5' -> 3')
R06N	GGAGGACGAGATAGGTTGGTGGGATTCCTG GTGGTGAGGC
R06M	GGAGGACGAGATAGGTTGGTGGGATTCCTG GTGGTAAGGC

Red letters represent binding regions between PNA probes and DNA stands.

Figure 3.7 (A) Array layout. (B) and (C) the scanned images of DNA sensors for R06 normal/mutant after washing with normal condition and high stringency washing. (D) and (E) Signal intensities of normal and high-stringency-washing condition derived from scanned images *via* the ImageJ image processing software. (F) The tables showing PNA and DNA sequences used in single-base mismatch discrimination experiment.

3.4.2 Sensitivity of the DNA sensor

To determine the detection limit, defined as the lowest concentration that signal intensity was significantly different form background, the HLA*B 5801 PNA-DNA duplex was observed by varying the DNA concentration in the range of 0.2 to 7 μM (**Figure 3.8B**). The detection limit was 200 nM (3.3 pmol/spot), as confirmed by the student's t-test (**Figure 3.8C**). The result herein (~40 ng) was comparable to previous reports[32] of the related dye (methylene blue) showing 40 ng as the detection limit in the gel format.

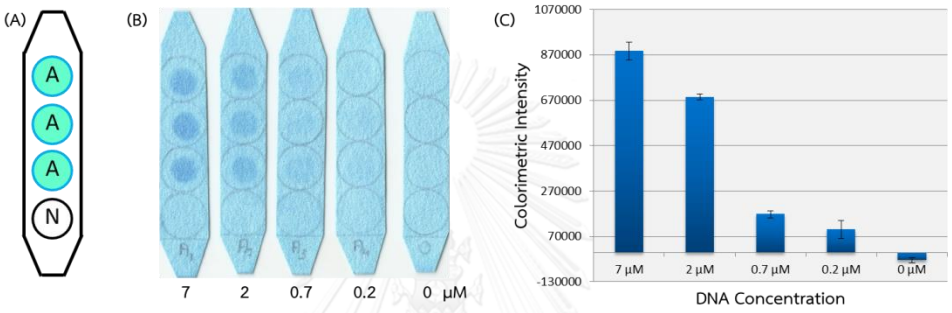

A = PNA 5801 N = negative control (no PNA)

(D)

PNA NAME	Sequence (N -> C)
5801	CTCCGTCCTCG - Lys

DNA NAME	Sequence (5' -> 3')
5801	CGAGGACGGAGCCCCGGGCGCCATGGAT AGAGCAGGAGGGG

Red letters represent binding regions between PNA probes and DNA stands.

Figure 3.8 (A) Array layout. (B) The scanned images of DNA sensors for HLA-B*5801 varied from 0 to 7 μM. (C) Signal intensities derived from scanned images *via* the ImageJ image processing software. (D) The tables showing PNA and DNA sequences used for determining detection limit.

3.4.3 The effect of DNA target structure on signal intensity

3.4.3.1 Effect of the location of binding region on the signal intensity

Three different sequences of DNA (DNA **A**, **B** and **C**) were designed with similar binding segments at different locations (**Figure 3.9A** and **D**). We found that **A**, in which the PNA binding region was located at the 5'-end interact most favorably with the immobilized acpcPNA, providing great signal intensity due to a less steric effect from a hanging part (**Figure 3.9C** and **E**). Like **A**, the binding region of **C** is located at the terminal of the DNA strand but at the opposite end (3'-end). Nevertheless, in this case the extra hanging sequence will be forced to stay close to surface because of the antiparallel binding direction with the immobilized PNA probes, thus inducing a steric hindrance which resulted in lower signal intensity than A. In a case of **B**, the binding segment at middle causes the most steric effect leading to lowest signal intensity. Thus, steric effect form hanging sequence was a major effect on the performance of this acpcPNA macroarray, whereas steric effect between the extra hanging sequence and the membrane surface showed only minor effects.

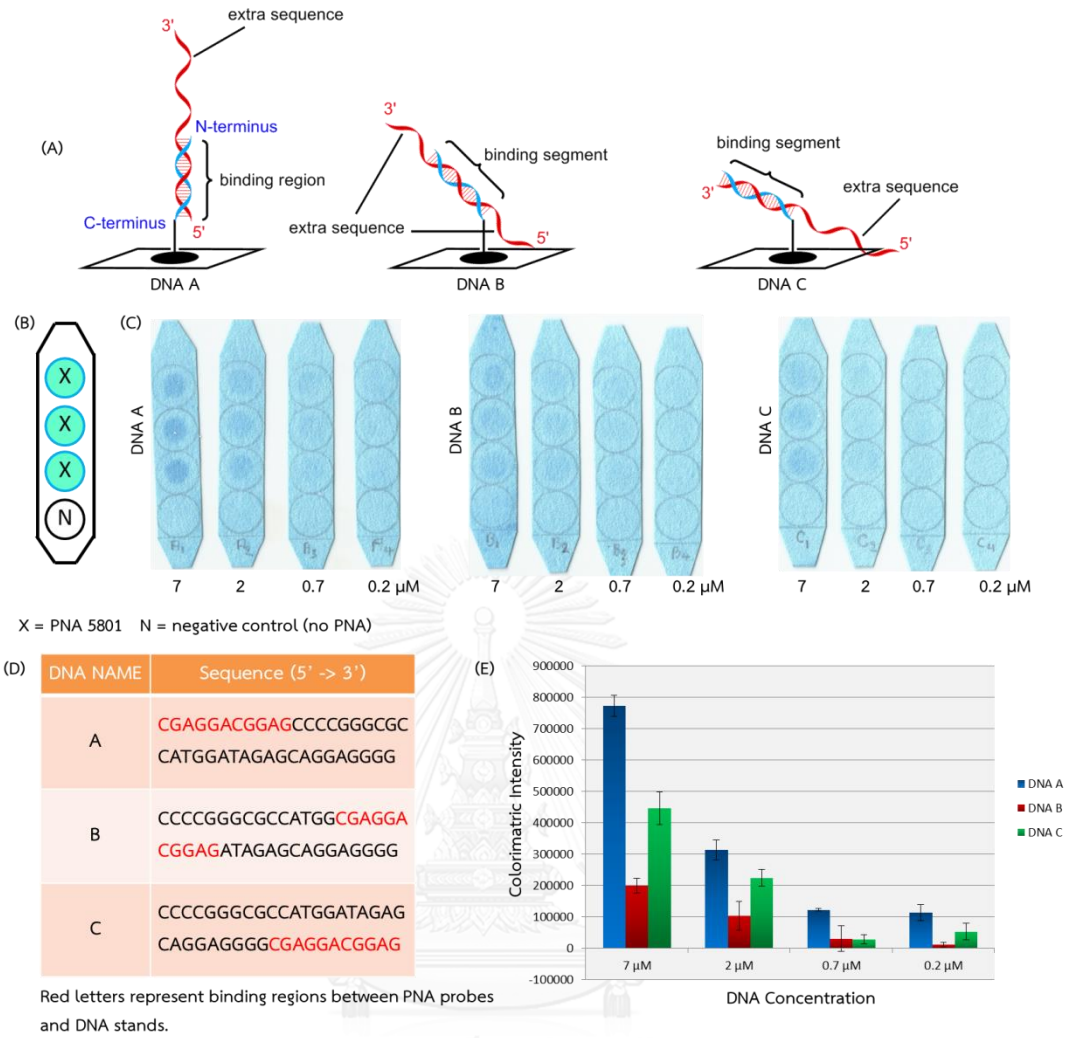

Figure 3.9 (A) The three forms of DNA-PNA hybrid on the membrane. (B) Array layout. (C) The scanned images of sensor incubated in three different DNAs. (D) The table showing the sequences of three DNAs used in this experiment. (E) Numerical values of signals in (C) as quantified by ImageJ.

3.4.3.2 Effect of lengths of hanging sequences on the signal intensity

It is generally accepted that longer DNA sequence has higher negative charge density leading to higher signal intensity due to increasing number of dye-binding sites.[33] To prove this concept, we created three sequences of DNA with different length of hanging segments (20, 30, and 40 bases) but contained the same binding sequence in order to control the binding energy (**Figure 3.10C**). Comparing between **A** and **B**, higher intensity of **A** confirmed the assumption (**Figure 3.10B** and **D**). However, more steric effect form sequence **C** (51 bases) caused lower signal intensity.

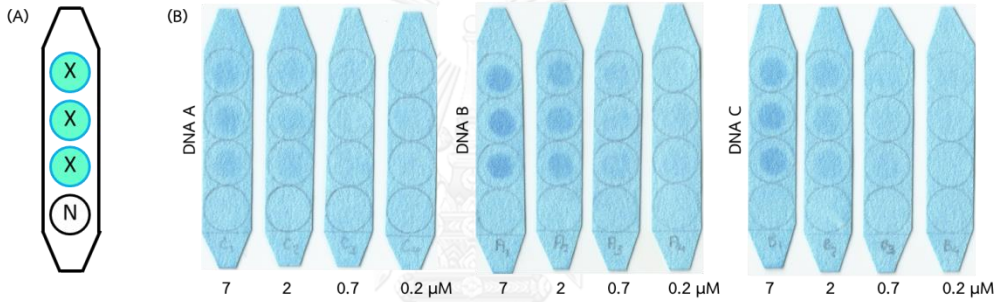

X = PNA 5801 N = negative control (no PNA)

(C)

DNA NAME	Sequence (5' -> 3')	DNA length
A	CGAGGACGGAGCCCCGGGCGC CATGGATAGA	31 bases
B	CGAGGACGGAGCCCCGGGCGC CATGGATAGAGCAGGAGGGG	41 bases
C	CGAGGACGGAGCCCCGGGCGC CATGGATAGAGCAGGAGGGGT AGGAACGCG	51 bases

Red letters represent binding regions between PNA probes and DNA stands.

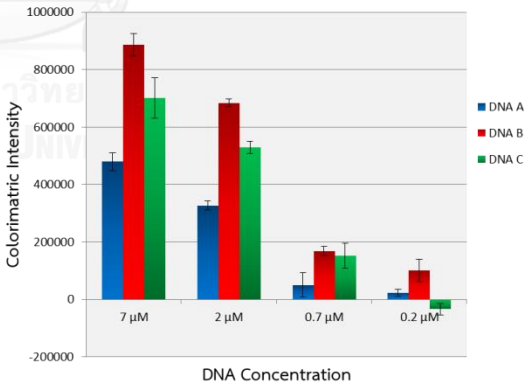

Figure 3.10 (A) Array layout. (B) The scanned images of sensor incubated in three different DNAs. (C) The table showing the sequences of three DNAs used in this experiment. (D) Numerical values of signals in (B) as qualified by ImageJ.

3.4.4 Comparison to DNA macroarray

DNA macroarray was prepared by immobilizing 3'-amino-linked DNA 5801 (**Figure 3.11E**) onto DVS-activated cellulose paper with the same strategy as PNA macroarray. Comparison of binding interaction between PNA 5801 and amino-linked DNA 5801 was performed via the same protocol, as judged by the signal intensity. It was clear that PNA could capture DNA targets more effectively in this condition (**Figure 3.11B** and **D**). According to previous reports, acpcPNA-DNA duplex was more thermally stable than DNA-DNA duplex. Therefore, this result confirmed that acpcPNA macroarray with the stronger binding affinity of acpcPNA probes provided higher sensitivity than did DNA macroarray.

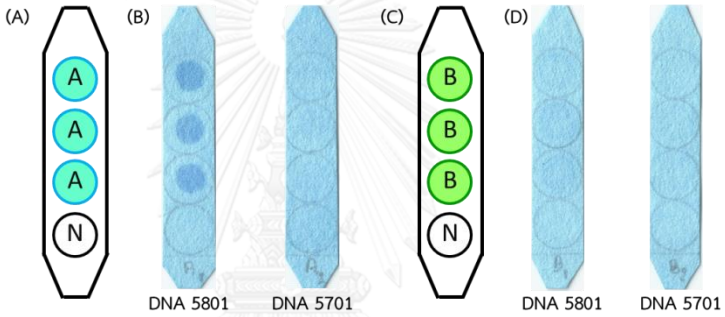

(E)

PNA probes NAME	Sequence (N -> C)
5801	CTCCGTCCTCG - Lys

DNA probes NAME	Sequence (5' -> 3')
5801	CTCCGTCCTCG – $(CH_2)_6$-NH_2

Target DNA NAME	Sequence (5' -> 3')
5801	CGAGGACGGAGCCCCGGGCGCCATGGATAGAGCAGGAGGGG
5701	CGAGGACGGAGCCCCGGGCGCCATGGATAGAGCAGGAGGGG

Red letters represent binding regions between PNA probes and DNA stands.

Figure 3.11 (A) PNA macroarray layout. (B) The scanned images of PNA macroarray for detecting DNA 5801. (C) DNA macroarray layout. (D) The scanned images of DNA macroarray for detecting DNA 5801. (E) The tables showing PNA and DNA sequences used in this experiment.

3.4.5 Attempts to improve sensitivity of the sensors by other DNA binding dyes

DNA-binding dyes such as ethidium bromide and SYBR Gold were generally used for staining DNA in gel electrophoresis. To compare with azure A, ethidium bromide and SYBR Gold were applied with this device under similar hybridization condition. Ethidium bromide binds to double-stranded DNA by intercalating,[34] so it is not ideal for detection of single-stranded DNA (**Figure 3.12A**). SYBR Gold is more sensitive than ethidium bromide for detecting double-stranded DNA and should be, in principle, much more sensitive for single-stranded DNA.[35] However, target DNA could not be detected in both circumstances (**Figure 3.12B**). It was explained that ethidium bromide did not intercalate effectively to short acpcPNA-DNA hybrid (11 base pairs), thus providing very low signal whereas SYBR gold staining resulted in a high background from non-specific interaction of this dye with the DVS-modified surface.

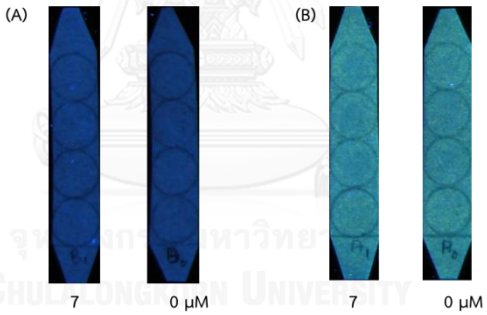

Figure 3.12 Photos of DNA sensors applied with (A) ethidium bromide and (B) SYBR Gold for DNA 5801.

3.4.6 PCR product

The 600-base pair PCR samples consisting of normal and Hb E sequences were obtained from Thalassemia Research Center, Mahidol University. Normal sequence was specific to PNA R06N when Hb E amplicon was specific to PNA R06M. Before hybridization, PCR products was denatured at 97 °C and quenched in ice bath to keep single strand form. No signal in both cases indicated that hybridization condition may not be optimal for PCR product which was similar to a case of DNA **C** (experiment in 3.4.3.2). Thus, condition for detecting long-length DNA and PCR product will need to be optimized further, in which additional spacer,[36-37] hybridization temperature[23] and salt concentration[21-22, 38] of hybridization buffer will be explored.

3.4.7 Comparison to other label-free DNA sensors

In this work, label-free detection of DNA using acpcPNA probes was performed under simple cationic dye staining. The advantages of this sensor were high specificity and minimal number of steps required. A comparison with similar works is shown in **Table 3.2** in terms of specificity, sensitivity and number of steps required. The dot-blot hybridization using acpcPNA probes by Laopa[16] and an aegPNA array for label-free detection of DNA using gold nanoparticle and gold enhancement[24] were chosen as comparators. AcpcPNA exhibited high specificity in both dot blot hybridization and this work, while single mismatch discrimination was not demonstrated in aegPNA array. In terms of sensitivity, the present work showed somewhat poorer detection limit than other techniques. This is limited by the detection method using cationic dye staining, which showed poor sensitivity. However, the simple two-step detection required for this DNA sensor as well as its excellent specificity suggest its potential to be utilized in point-of-care test. The detection method still needs improvement, and perhaps used in combination with a suitable signal enhancement method to improve the sensitivity even further.

Table 3.2 Comparison with similar reports in terms of specificity, sensitivity and number of required steps.

Parameters	This work	Dot blot hybridization using acpcPNA probes[16]	AegPNA array using gold nanoparticle and gold enhancement[24]
Specificity	Single base discrimination	Single base discrimination	Non-complementary discrimination
Sensitivity	200 nM (3.3 pmol)	10 fmol	10 pM
Number of step required for the detection	2 steps (hybridization and cationic dye staining, at least 50 minutes)	4 steps (DNA attachment, hybridization, conjugation with secondary probe and enzymatic detection, at least 1.25 hour)	3 steps (hybridization, AuNP staining and gold enhancement, at least 1.7 hours)

CHAPTER IV
CONCLUSION

In this work, a new DNA sensor based on acpcPNA macroarray was developed by immobilization of acpcPNA on DVS-activated cellulose paper. The hybridization was rapidly performed through capillary transport of DNA sample solution. The label-free DNA detection was carried out by a simple staining with cationic-dye. Preliminary tests demonstrated the achievement of fabrication of acpcPNA macroarray, capillary transport hybridization and detection method. In terms of specificity, this sensor can discriminate fully complementary DNA from double-base mismatch DNA under normal condition and from single-base mismatch DNA by employing a more stringent washing. The detection limit was 200 nM which could have been theoretically raised by increasing a length of DNA target. However, the steric effect was higher along with the length of DNA strand. The favorable location of the PNA binding region was a 5'-terminal end because of a less steric effect. The comparison between acpcPNA and DNA macroarrays indicated that sensitivity of acpcPNA macroarray was better, but still on the poor side compared to other PNA-based macroarrays that incorporated a signal amplification mechanism.

This study provided acpcPNA macroarray with a promising performance in term of selectivity and ease of use. Analysis of real DNA samples obtained from PCR will require further optimization before it can be developed into a practical device for general diagnostic applications.

REFERENCES

References:

1. Divne, A.-M.; Allen, M. *Forensic Sci. Int.* **2005**, *154*, 111-121.
2. Sforza, S.; Corradini, R.; Tedeschi, T.; Marchelli, R. *Chem. Soc. Rev.* **2011**, *40*, 221-232.
3. Booth, S. A.; Drebot, M. A.; Tipples, G. A.; Ng, L. K. *Can. J. Infect. Dis.* **2000**, *11*, 291-294.
4. Miller, M. B.; Tang, Y.-W. *Clin. Microbiol. Rev.* **2009**, *22*, 611-633.
5. Yoo, S. M.; Choi, J. H.; Lee, S. Y.; Yoo, N. C. *J Microbiol Biotechnol* **2009**, *19*, 635-46.
6. Heller, M. J. *Annu. Rev. Biomed. Eng.* **2002**, *4*, 129-153.
7. Jirakittiwut, N.; Panyain, N.; Nuanyai, T.; Vilaivan, T.; Praneenararat, T. *RSC Advances* **2015**, *5*, 24110-24114.
8. Araújo, A. C.; Song, Y.; Lundeberg, J.; Ståhl, P. L.; Brumer, H. *Anal. Chem.* **2012**, *84*, 3311-3317.
9. Yu, A., et al. *Langmuir* **2012**, *28*, 11265-11273.
10. Liana, D. D.; Raguse, B.; Gooding, J. J.; Chow, E. *Sensors* **2012**, *12*, 11505.
11. Parolo, C.; Merkoci, A. *Chem. Soc. Rev.* **2013**, *42*, 450-457.
12. von Lode, P. *Clin. Biochem.* **2005**, *38*, 591-606.
13. Song, Y.; Gyarmati, P.; Araújo, A. C.; Lundeberg, J.; Brumer, H.; Ståhl, P. L. *Anal. Chem.* **2014**, *86*, 1575-1582.
14. Saikrishnan, D.; Goyal, M.; Rossiter, S.; Kukol, A. *Anal. Bioanal. Chem.* **2014**, *406*, 7887-7898.
15. Shi, H., et al. *Biosens. Bioelectron.* **2015**, *66*, 481-489.
16. Laopa, P. S.; Vilaivan, T.; Hoven, V. P. *Analyst* **2013**, *138*, 269-277.
17. Nielsen, P.; Egholm, M.; Berg, R.; Buchardt, O. *Science* **1991**, *254*, 1497-1500.

18. Lundin, K. E.; Good, L.; Strömberg, R.; Gräslund, A.; Smith, C. I. E. Biological Activity and Biotechnological Aspects of Peptide Nucleic Acid. in Jeffrey C. Hall, J. C. D. T. F.; Veronica van, H. (eds.),Advances in Genetics, pp. 1-51: Academic Press, 2006.

19. Shakeel, S.; Karim, S.; Ali, A. *J. Chem. Technol. Biotechnol.* **2006**, *81*, 892-899.

20. Egholm, M.; Buchardt, O.; Nielsen, P. E.; Berg, R. H. *J. Am. Chem. Soc.* **1992**, *114*, 1895-1897.

21. Choi, J.-J.; Jang, M.; Kim, J.; Park, H. *J Microbiol Biotechnol* **2010**, *20*, 287-293.

22. Choi, J.-j.; Kim, C.; Park, H. *J. Clin. Microbiol.* **2009**, *47*, 1785-1790.

23. Geiger, A.; Lester, A.; Kleiber, J.; Ørum, H. *Nucleos. Nucleot.* **1998**, *17*, 1717-1724.

24. Kim, S. K.; Cho, H.; Jeong, J.; Kwon, J. N.; Jung, Y.; Chung, B. H. *Chem. Commun.* **2010**, *46*, 3315-3317.

25. Singh, R. P.; Oh, B.-K.; Choi, J.-W. *Bioelectrochemistry* **2010**, *79*, 153-161.

26. Vilaivan, T. *Acc. Chem. Res.* **2015**, *48*, 1645-1656.

27. Lowe, G.; Vilaivan, T. *Journal of the Chemical Society, Perkin Transactions 1* **1997**, 547-554.

28. LePlae, P. R.; Umezawa, N.; Lee, H.-S.; Gellman, S. H. *The Journal of Organic Chemistry* **2001**, *66*, 5629-5632.

29. Vilaivan, T.; Srisuwannaket, C. *Org. Lett.* **2006**, *8*, 1897-1900.

30. Santos, F. R.; Bianchi, N. O.; Pena, S. D. *Genome Res.* **1996**, *6*, 601-611.

31. Boontha, B.; Nakkuntod, J.; Hirankarn, N.; Chaumpluk, P.; Vilaivan, T. *Anal. Chem.* **2008**, *80*, 8178-8186.

32. Mülhardt, C.; Beese, E. W. The Tools. in Molecular Biology and Genomics, pp. 37-63. Burlington: Academic Press, 2007.

33. Klein, F.; Szirmai, J. A. *Biochim. Biophys. Acta, Spec. Sect. Nucleic Acids Relat.* **1963**, *72*, 48-61.

34. Olmsted, J.; Kearns, D. R. *Biochemistry* **1977**, *16*, 3647-3654.

35. Tuma, R. S., et al. *Anal. Biochem.* **1999**, *268*, 278-288.

36. Oh, S. J., et al. *Nucleic Acids Res.* **2005**, *33*, e90.

37. Dimitrios, S. E.; Penelope, C. I.; Theodore, K. C. *Nanotechnology* **2011**, *22*, 155501.

38. Ananthanawat, C.; Vilaivan, T.; Hoven, V. P.; Su, X. *Biosensors and Bioelectronics* **2010**, *25*, 1064-1069.

APPENDIX

Characterization of acpcPNAs

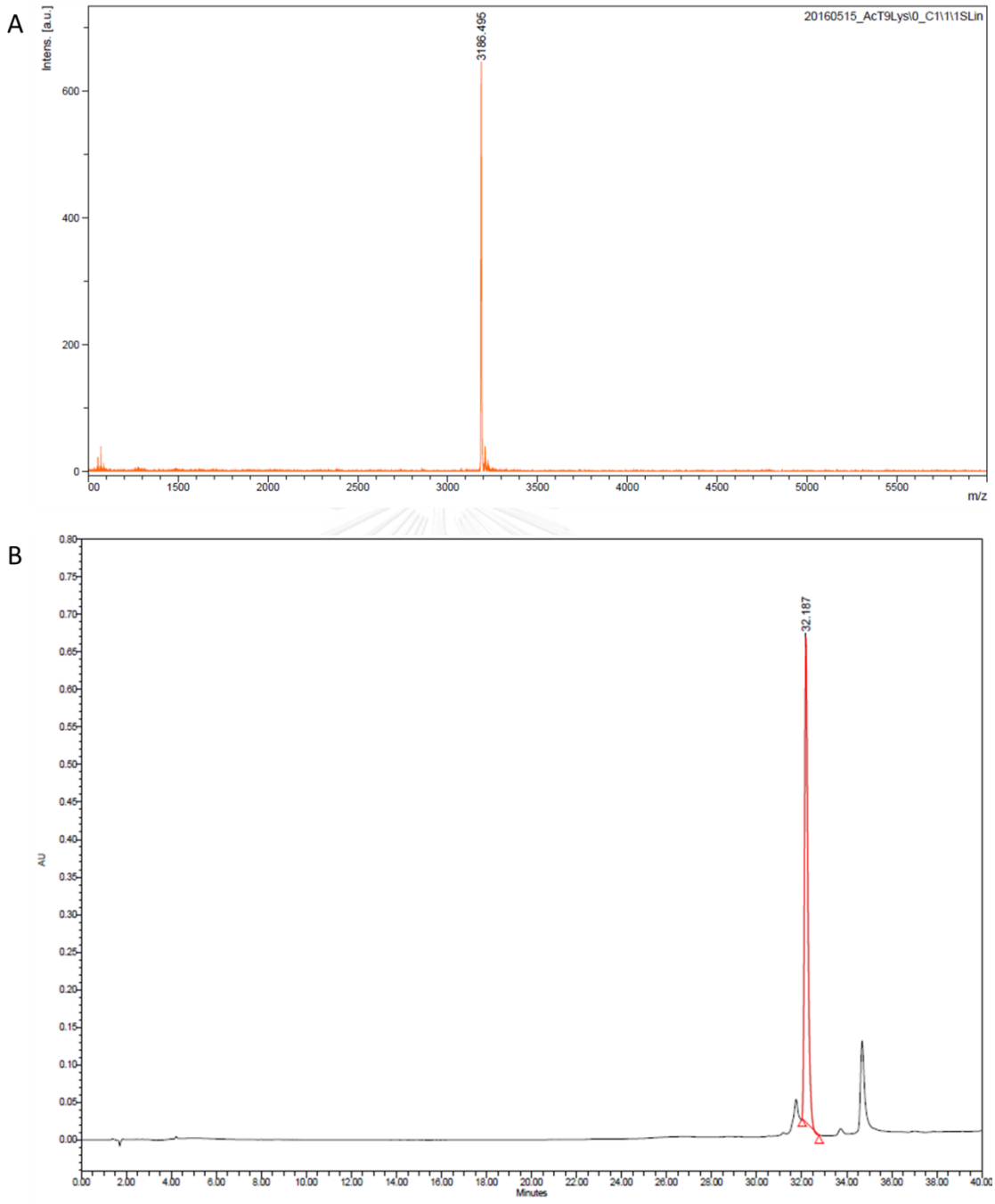

Figure A1 (A) Mass spectrum and (B) chromatogram of PNA T_9.

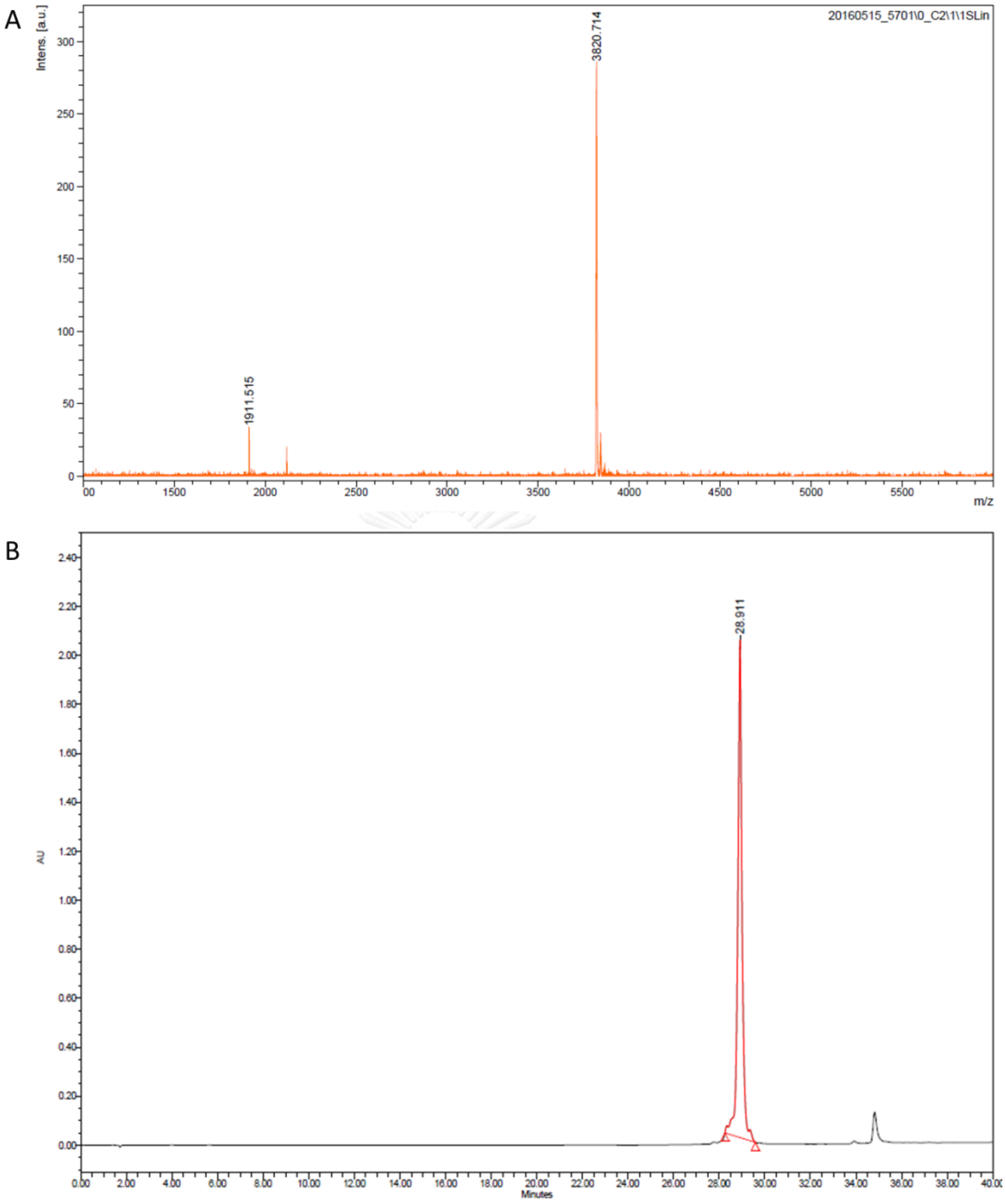

Figure A2 (A) Mass spectrum and (B) chromatogram of PNA 5701.

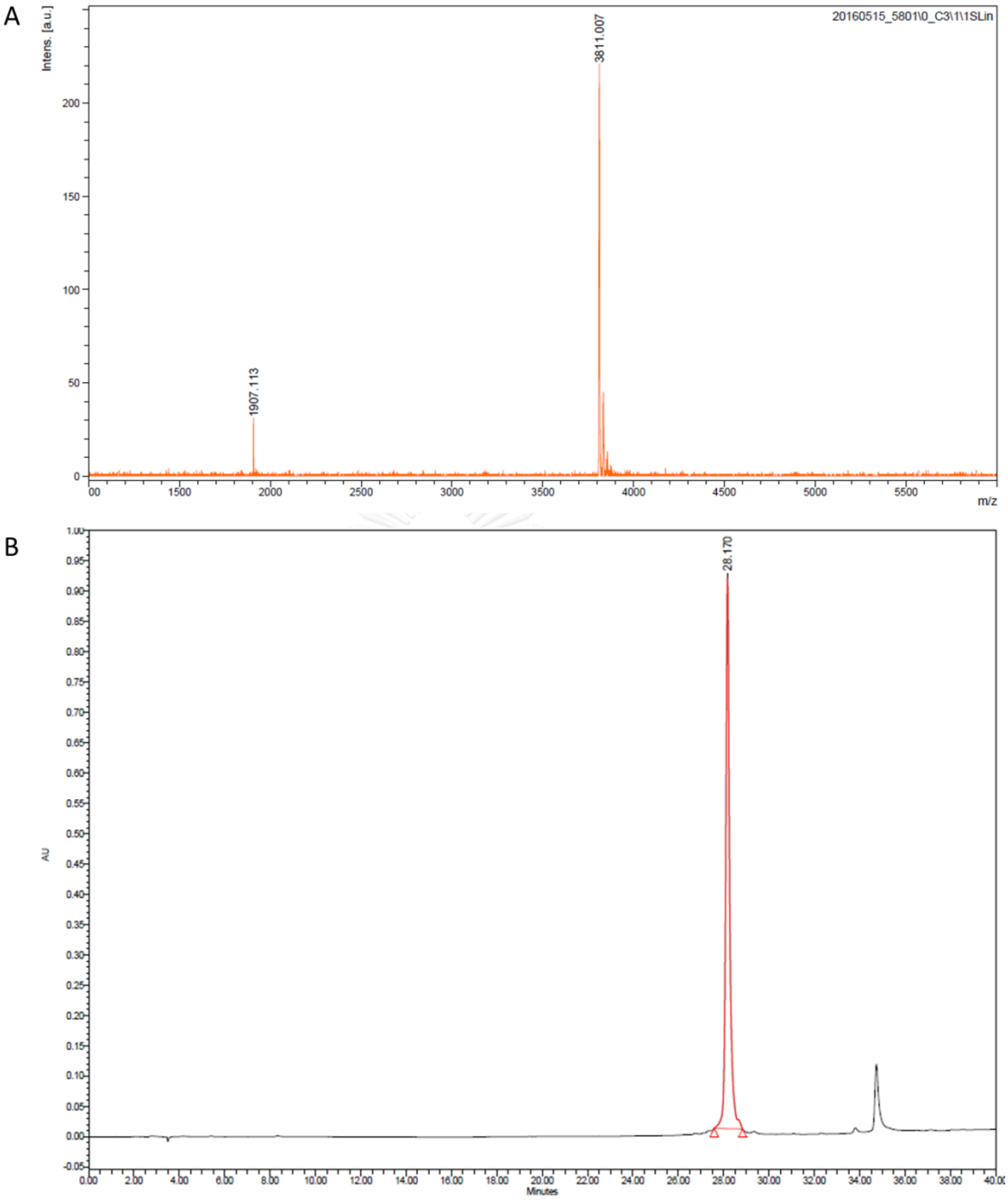

Figure A3 (A) Mass spectrum and (B) chromatogram of PNA 5801.

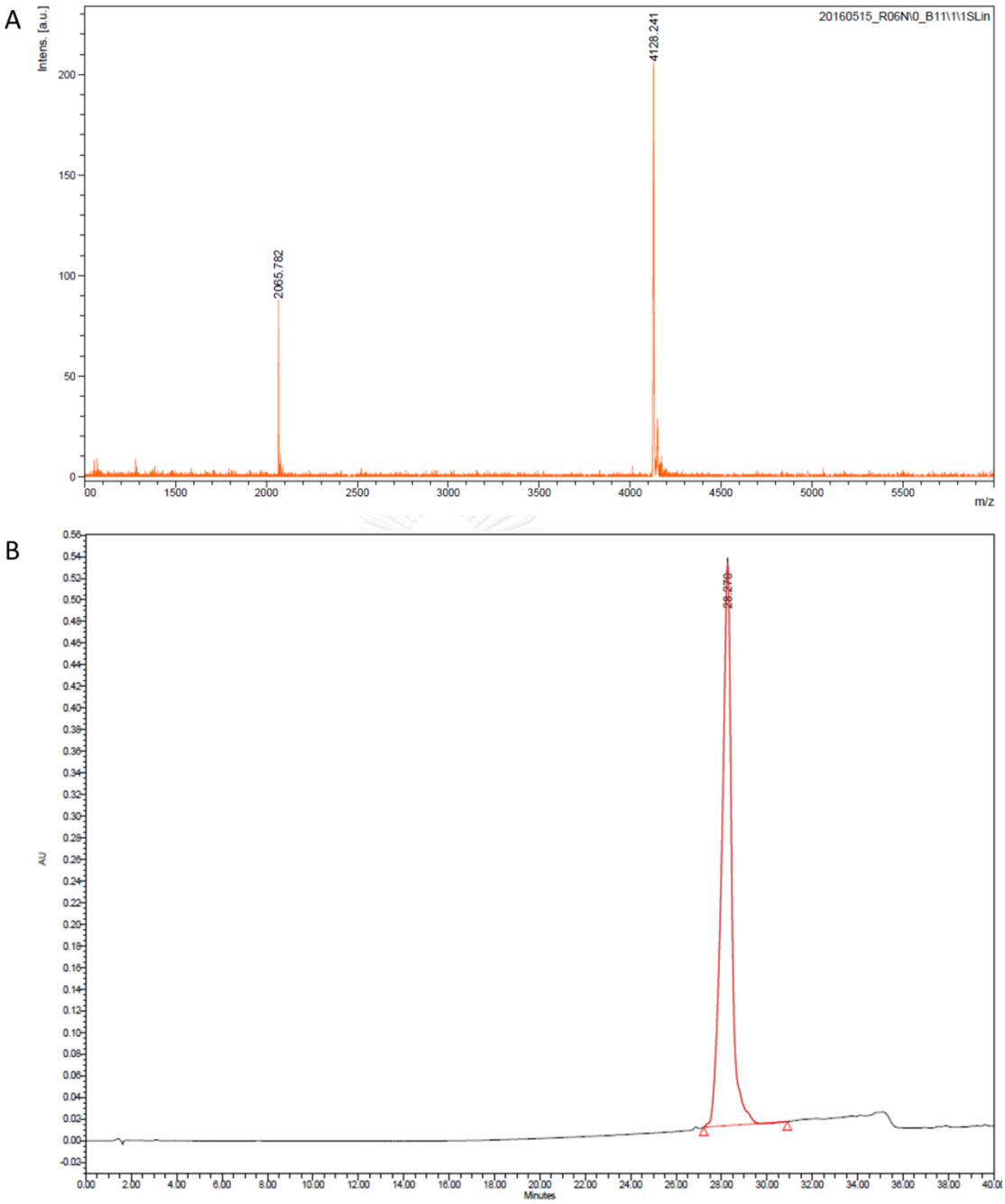

Figure A4 (A) Mass spectrum and (B) chromatogram of PNA R06N.

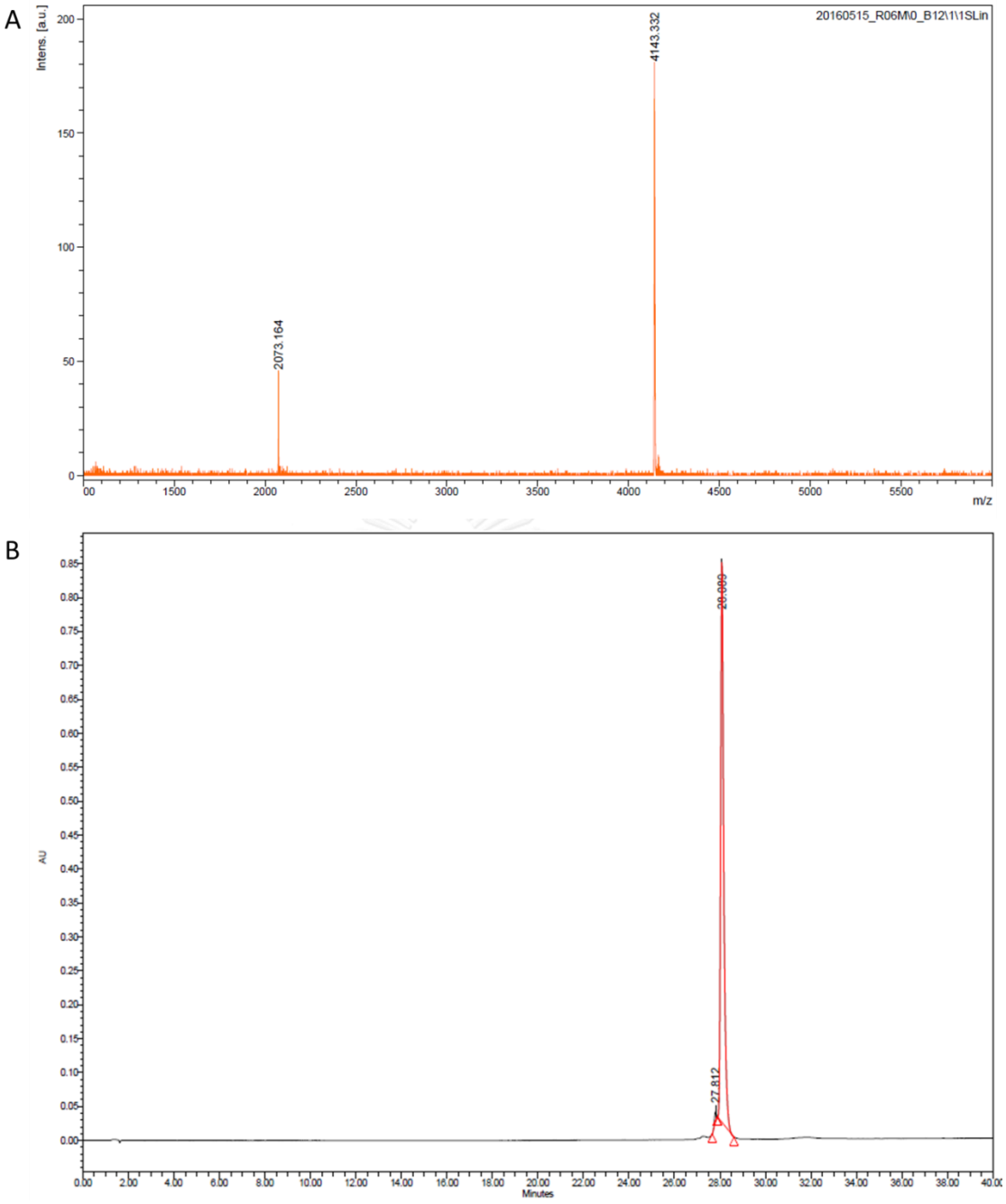

Figure A5 (A) Mass spectrum and (B) chromatogram of PNA R06M.

Click chemistry for preparation of acpcPNA-immobilized cellulose paper

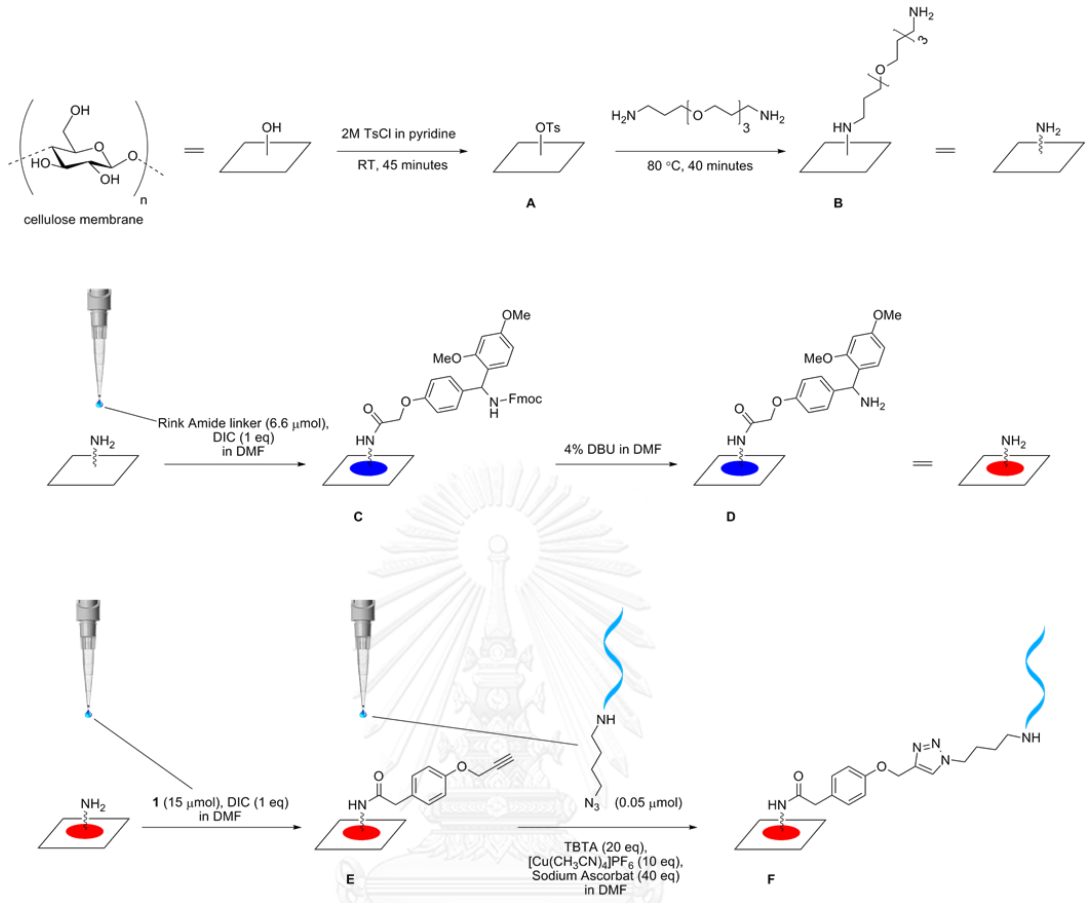

Figure A6 Schematic illustration of the methodology of preparation of acpcPNA-immobilized cellulose paper *via* click reaction.

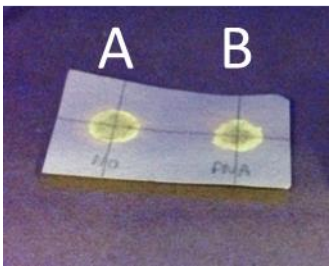

Figure A7 Fluorescece images of (A) membrane **F** without acpcPNA and (B) membrane **F**.

Fmoc quantification protocol

The loading of Rink amide linker on membrane **C** was determined by UV quantification of the cleaved Fmoc protecting group. A piece of membrane **C** (0.28 cm^2) was incubated in 4% DBU in DMF for 15 minutes. The absorbance was then measured at 296 nm (ε_{296} = 9880 $M^{-1}cm^{-1}$). The loading of Rink amide linker was in the range of 0.2–1 μmol/cm^2.

Immobilization of acpcPNA onto cellulose by using disuccinimidyl adipate

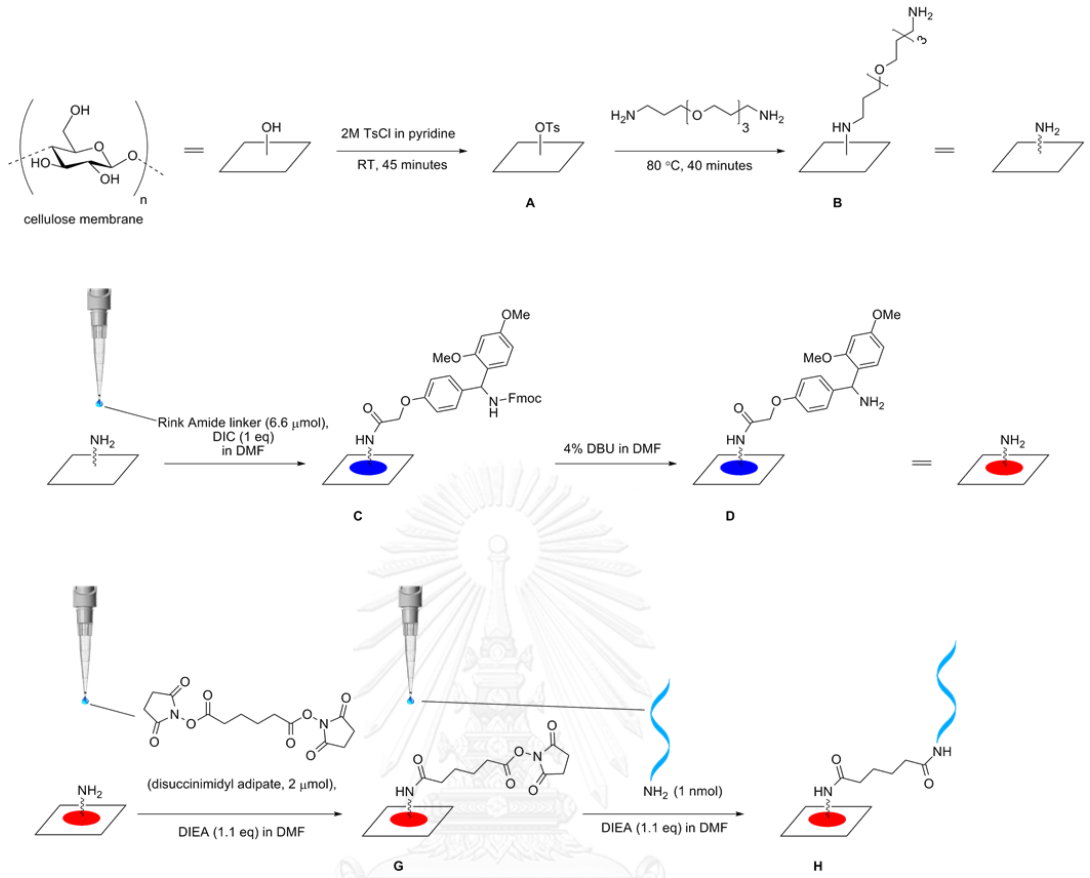

Figure A8 Scrematic illustration of the methodology of preparation of acpcPNA-immobilized cellulose paper using disuccinimidyl adipate as a linker.

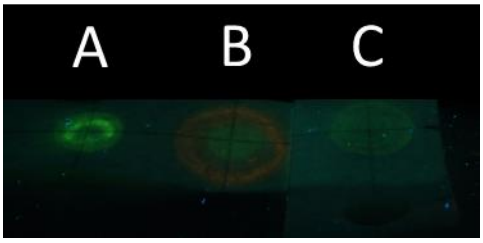

Figure A9 Fluorescence images of acpcPNA(T_9, 1 nmol)-immobilized cellulose membrane after hybridization (spotting DNA solution onto the membrane) with (A) fluorescein-labeled complementary (sequence: 5'-fluorescein-AAAAAAAAA-3', 1 nmol) and (B) TAMRA-labeled non-complementary DNA (5'-TAMRA-CGAGGGATAACT-3', 1 nmol) and (C) negative control (without acpcPNA).

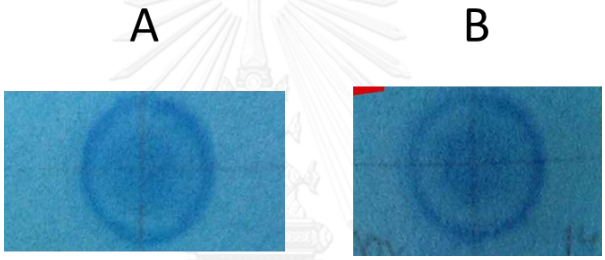

Figure A10 Methylene blue staining of acpcPNA(T_9, 1 nmol)-immobilized cellulose membrane after hybridization (spotting DNA solution onto the membrane) with (A) fluorescein-labeled complementary DNA (sequence: 5'-AAAAAAAAA-3', 1 nmol) and (B) negative control (without DNA).

Immobilization of acpcPNA onto PDITC-activated cellulose membrane

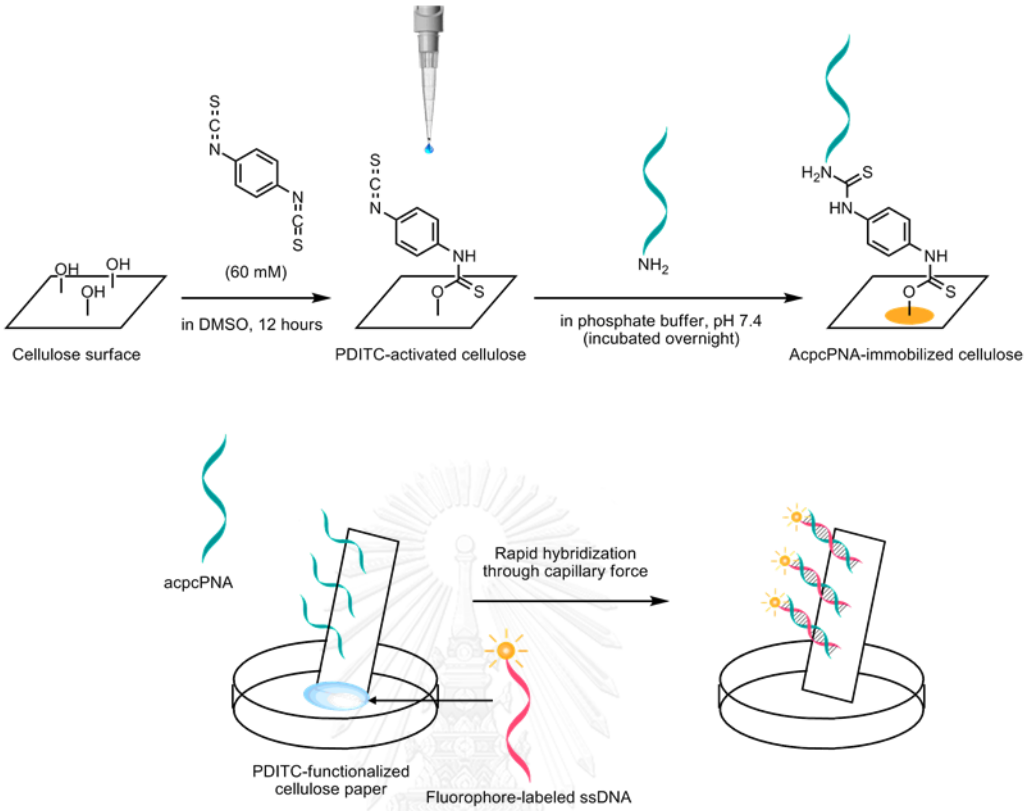

Figure A11 Schematic illustration of the methodology of immobilization of acpcPNA PDITC-activated cellulose paper and rapid hybridization of target DNA through capillary force.

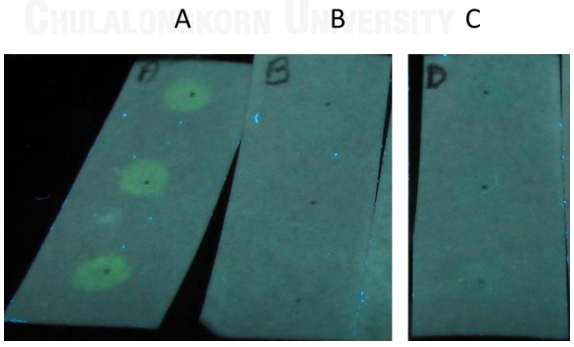

Figure A12 Fluorescence images of acpcPNA(T_9, 100 pmol)-immobilized cellulose memmbrane after hybridization (capillary transport) with (A) fluorescein-labeled complementary (sequence: 5'-fluorescein-AAAAAAAAA-3', 2 μM) and (C) TAMRA-labeled non-complementary DNA (5'-TAMRA-CGAGGGATAACT-3', 2 μM) and (B) negative control (without acpcPNA).

Silver Staining

After hybridization (spotted DNA solution onto acpcPNA-immobilized paper and then washed in PBST), the strip was immersed in $AgNO_3$ solution (0.5 mg/mL) for 10 minutes. The membrane was washed with MilliQ water for 3 minutes twice, incubated in the mixture of 1.5% NaOH and 0.1% formaldehyde for 1 minute and finally washed with fixative solution containing 10% ethanol and 0.5% acetic acid for 10 minutes.

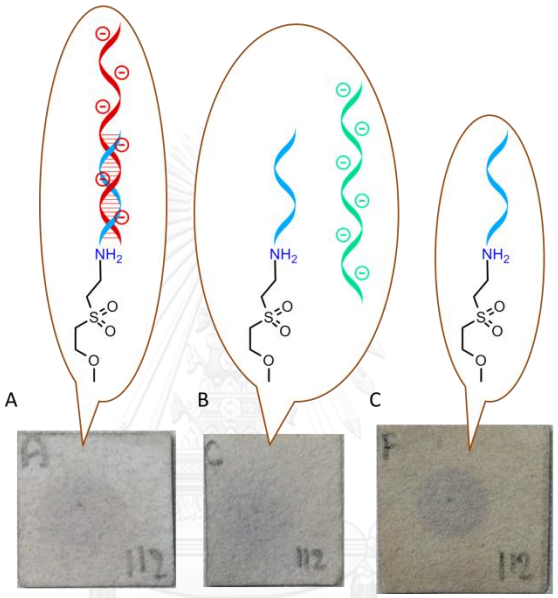

Figure A13 Optical images of acpcPNA(T_9, 100 pmol)-immobilized cellulose memmbrane after hybridization (spotting DNA solution onto the membrane) with (A) complementary DNA (sequence: 5'-CGCGGCGTACAAAAAAAAAGCATGCCCTGG-3', 50 pmol) and (B) non-complementary DNA (sequence: 5'-CGCGGCGTACAGTG ATCTACGCATGCCCTGG-3', 50 pmol) and (C) negative control (without DNA).

Gold nanoparticle (AuNP) staining with gold enhancement

After hybridization (spotted DNA solution onto acpcPNA-immobilized paper and then washed in PBST), the strip was incubated in AuNP solution (synthesized by Dr. Prompong Pienpinijtham) for 30 minutes and then immersed in gold enhancement solution purchased from Nanoprobes, Inc. for 5 minutes. The membrane was washed with DI water for 3 minutes.

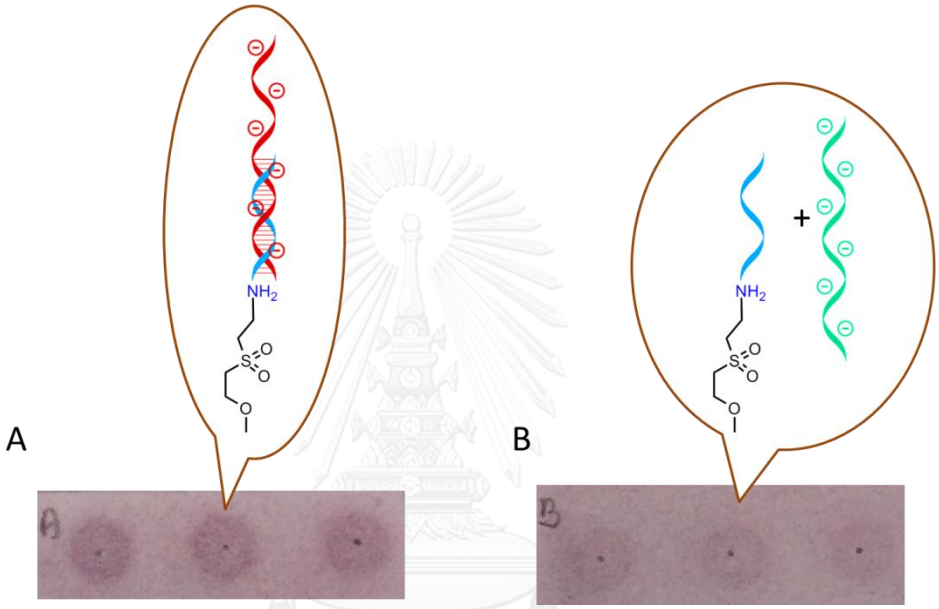

Figure A14 Optical images of acpcPNA(T_9, 100 pmol)-immobilized cellulose membrane after hybridization (spotting DNA solution onto the membrane) with (A) complementary DNA (sequence: 5'-CGCGGTCGACGGTCACGTACGAAAAAAAAA-3', 100 pmol) and (B) non-complementary DNA (sequence: 5'-CGCGGCGTACAGTGA TCTACCATGCCCTGG-3', 100 pmol).

Screening cationic dyes for DNA detection

After hybridization (spotted DNA solution onto the left column of acpcPNA-immobilized paper and then washed in PBST), each strip was incubated in methylene blue (0.05 mg/mL), azure A (0.01% in 5% ethanol), azure II (0.01% 5% ethanol), ethyl violet (0.0008% in 0.18% ethanol) and nile blue (0.01% in 10% methanol) solutions for 5 minutes and then all of them were washed with DI water for 3 minutes (3 times).

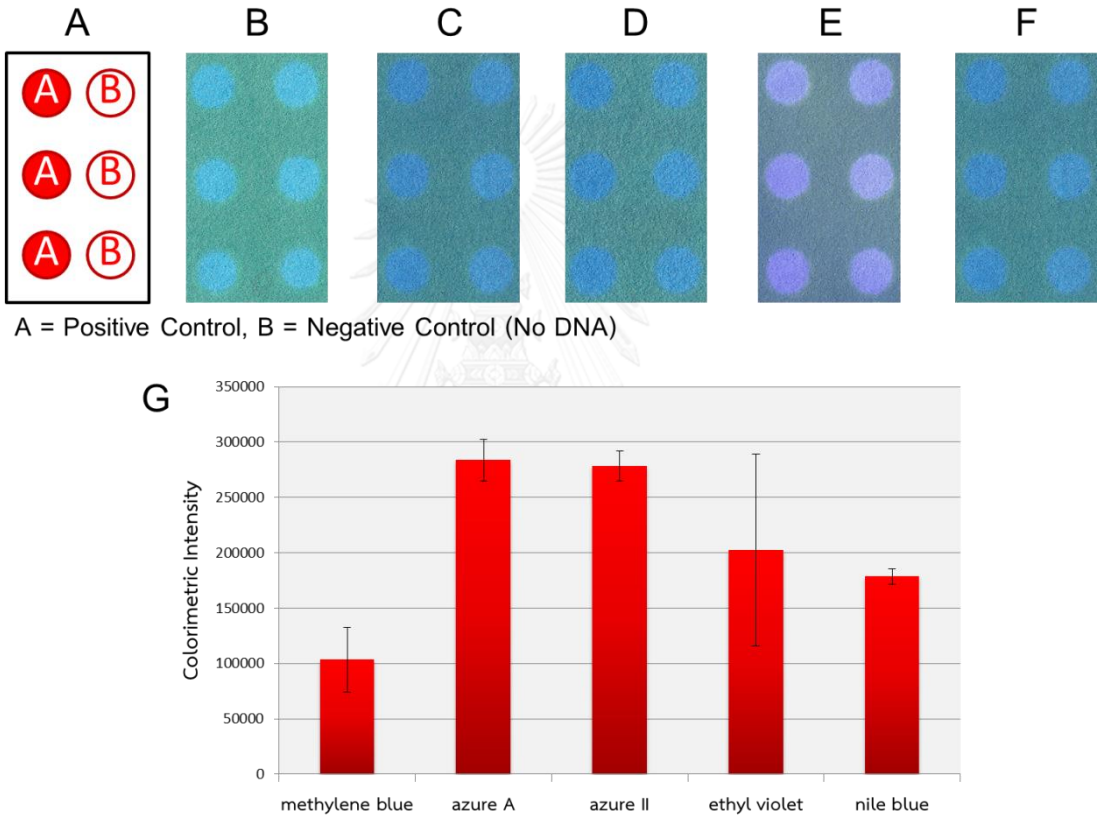

Figure A15 (A) Array layout. The scanned images of DNA sensors (T_9, 100 pmol/spot) after hybridization (spotting DNA solution onto the membrane) with complementary DNA (sequence: 5'-CGCGGTCGACGGTCACGTACGAAAAAAAAA-3', 100 pmol) and stained with (B) methylene blue, (C) azure A, (D) azure II, (E) ethyl violet and (F) nile blue solutions. (G) Signal intensities derived from scanned images *via* the ImageJ image processing software.

Detection of target DNA in DNA mixture

From a previous work[16], the limitation was a competition among different DNAs in absorbing on membrane rendering possibility that desired sequences cannot be detectable. This limitation is likely conquered by using this acpcPNA macroarray. DNA 5801 and DNA 5701 were mixed in other different DNAs, before detection method was performed. A result showed that only a case of DNA 5801 mixed in other DNAs gave a signal. The achievement of detection of target DNA in DNA mixture was therefore proved.

(A) (B) (C)

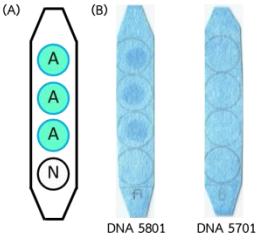

Target DNA NAME	Sequence (5' -> 3')
5801	CGAGGACGGAGCCCCGGGCGCCATGGATAGAGCAGGAGGGG
5701	CGAGGACGGAGCCCCGGGCGCCATGGATAGAGCAGGAGGGG
DNA mixture	CGT ACG
	AGT GAC TAC
	AGT GAC CTC TAC
	AAT TAC GAC ATC ATA
	GCA GTC AGT TGA CAC TGA
	AGC CTG CGG AAC CTG CGC GGC TAC TAC AAC
	TTTTTTTTT CAT GCA TAT ACG TAC TTTTTTTTT
	GTG CAG AGA TAT TAC ATG CAT CAT TGG GAG GGG GAA TCT
	CAC TAC TAA GGC TTC TTT CCC CTT CCC AAG TAG GGA TAG GTA AGA

PNA probes NAME	Sequence (N -> C)
5801	CTCCGTCCTCG - Lys

Figure A16 (A) Array layout. (B) the scanned images of DNA sensors for DNA 5801 in DNA mixture. (C) The tables showing PNA and DNA sequences used in detection target DNA contaminated by other DNAs.

VITA

I, Nuttapon Jirakittiwut, was born on the 20th of January 1991 in Chiang Mai. I got opportunity form Science Achievement Scholarship of Thailand to study in Chemistry Department, Chiang Mai University, Thailand. I received my Bachelor's Degree with first class honors from the Department of Chemistry, Faculty of Science, Chiang Mai University, Thailand in 2012. After effort during 2 years in Master's Degree, my research named "Pyrrolidinyl peptide nucleic acids immobilised on cellulose paper as a DNA sensor" was published in 2015.